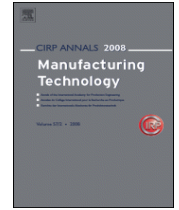


Contents lists available at [SciVerse ScienceDirect](https://www.sciencedirect.com)

# CIRP Annals Manufacturing Technology

Journal homepage: [www.elsevier.com/locate/cirp](http://www.elsevier.com/locate/cirp)

## Abrasive processes for micro parts and structures

J.C. Aurich (1)<sup>a</sup>, B. Kirsch<sup>a</sup>, D. Setti<sup>a</sup>, D. Axinte (1)<sup>b,c</sup>, A. Beaucamp (2)<sup>d</sup>, P. Butler-Smith<sup>b</sup>, H. Yamaguchi (2)<sup>e</sup><sup>a</sup> Institute for Manufacturing Technology and Production Systems, TU Kaiserslautern, Kaiserslautern, Germany<sup>b</sup> Faculty of Engineering, University of Nottingham, Nottingham, United Kingdom<sup>c</sup> Faculty of Science and Engineering, University of Nottingham, Ningbo, China<sup>d</sup> Department of Micro-Engineering, Kyoto University, Kyoto 606-8501, Japan<sup>e</sup> Department of Mechanical and Aerospace Engineering, University of Florida, 226 MAE-B, Gainesville, FL USA

Submitted by Jan C. Aurich

The demand for miniaturized products and functionalized parts is constantly increasing. Many such products and applications are machined by abrasive processes, particularly those made of hard and brittle materials. The first part of this keynote paper is dedicated to a discussion of micro parts and micro structures machined – at least in part - by abrasive processes. The second part contains a detailed presentation of the abrasive processes used to machine such micro parts and structures. The strengths and weaknesses of these processes, among others being dicing, micro grinding, micro abrasive blasting, and vibration and magnet field assisted finishing are discussed. The paper concludes with a discussion of future trends and research needs in the field.

Micro machining, Miniaturization, Micro structure

### 1. Introduction

The miniaturization and functionalization of products and parts has been one of the key aims of manufacturing research over a period of several decades and has been the topic of several CIRP keynote papers, most recently in 2006 [63]. Micro structures are used to provide unique properties to otherwise standard surfaces; they allow to reduce size and weight of products while integrating more functions – in summary they can help to bridge the gap between the macro and the nano scale [71]. Various CIRP keynote papers have dealt with micro structured surfaces and explored their properties [30,54,152,153,193], going back to the 1999 keynote paper that defined such structures [66].

While mass production technologies for micro structured surfaces are available, technologies to manufacture such structures on individual, one-of-a-kind specimens, have either significant limitations regarding the machinable materials and geometry or are prohibitively costly. There are many products and applications requiring hard and brittle materials as the base substrate. This class of materials is commonly processed via abrasive processes.

This keynote paper provides an overview of products and applications that need micro abrasive processes. These products either have sizes in the micro range or exhibit micro sized features or structures. Following this overview of products, current capabilities of abrasive processes for micro parts and structures are investigated in detail. This investigation is complemented by a section on modelling of such small-scale material removal processes, a promising technique to increase the understanding of underlying mechanisms.

Finally, the authors have summarized possible future trends and research needs in the area of abrasive processes for micro parts and structures.

### 2. Products and Applications

Micro-sized products manufactured or finished by applying abrasive processes cover various application fields such as microfluidics, biomedical systems, micro electro mechanical systems (MEMS), optics, the manufacturing of cutting tools, and the deburring of micro parts. In many of these areas, the fabrication of three-dimensional micro structures with distinct topographies is of great interest as well. This chapter introduces various typical products and applications, their properties and requirements.

#### 2.1 Microfluidic systems

Microfluidics is the science and technology of systems dealing with small amounts of fluids, typically nanolitres to picoliters. A typical microfluidic system consists of microchannels plus the associated drivers such as pumps, mixers, heaters, fluid-particle reservoirs, actuators, valves, sensors, controllers, etc. (Fig. 1)

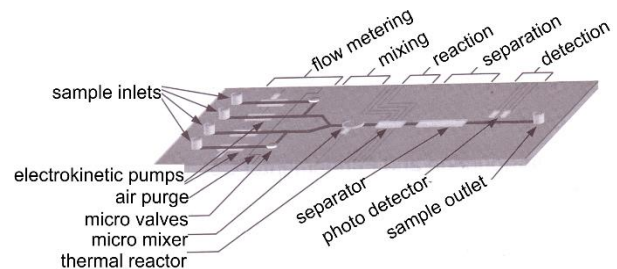
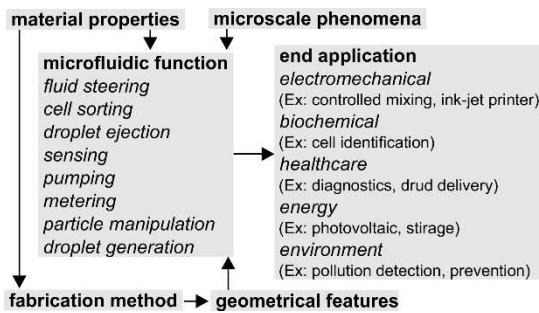


Fig. 1. Microfluidic system representation [121].



**Fig. 2.** Relational map among fabrication methods, geometric features, material properties, microscale phenomena, microfluidic functions, and end applications (based on [121,133]).

Microfluidic systems provide one or more microfluidic functions. According to [133], the manufacturing method has to be chosen to produce the required geometric features on appropriate materials to achieve the microfluidic functions as needed. Fig. 2 shows the interconnected relationship between manufacturing methods, geometric features, material properties, microfluidic functions, and end applications. According to [200,203], the shape of the micro channel cross section significantly affects the mixing performance of the micro mixer. Micro channels can have different cross sections such as rectangular, trapezoidal, semi-circle, and bell-shape. Besides the cross-section, the aspect ratio and the surface roughness decide upon the functions of microfluidic systems. The aspect ratio is defined as the ratio between micro structure height and width. For microfluidic systems, a high aspect ratio is very desirable for the performance of many sensors and actuators such as comb-drive actuators [133]. The manufacturing of structures with high aspect ratio is often challenging due to the extreme required anisotropy. While isotropic processes like wet etching cannot match this, micro grinding methods can overcome this issue as shown in Fig. 3.

In microfluidic systems, the manufacturing of microchannels with sufficient length, depth and the required level of surface finish is critical for its performance. The surface roughness of the channel surface significantly affects the wetting behaviour of liquids and the flow of fluid within the microchannel. In microfluidic applications that are based on surface chemistry and biomolecule interactions, a certain roughness can be advantageous due to the higher surface area between the fluid and the base substrate. However, a higher roughness may change the flow from laminar to turbulent; further it leads to a pressure drop [277]. Accordingly, one must select and optimize suitable process conditions for a given workpiece material. Substrate materials used for micro pumps are glass [208,265,266], silicon [232] or polymethylmethacrylate (PMMA) and [262,263,265,267] various types of glass substrates [20,84,123,129,189,202,205,214,231,259] for electrophoresis microchips.

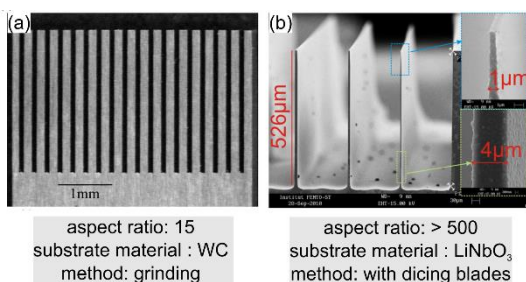


**Fig. 3.** Examples of high aspect ratio anisotropic structures produced on various substrates [56,192].

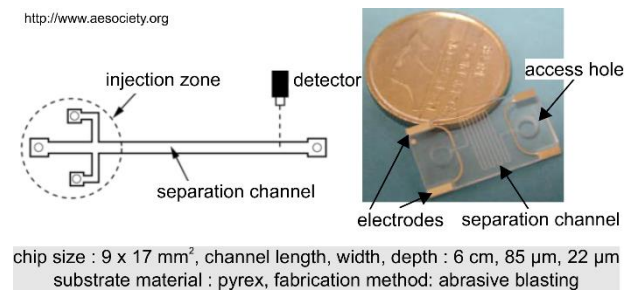


**Fig. 4.** An example of finished electrophoresis chip [205].

### 2.1.1 Capillary electrophoresis chips

Several chemical and biomedical analysis methods consist of the sequence of phases classified as sample preparation, reaction and product analysis. As the reaction phase has to deal with multiple chemical species, the later analysis phase must be capable of separating and identifying the individual components. Electrophoresis works on the principle of inducing detectable differences in the migration behaviour between charged chemical species under the influence of an applied electric field. This offers great potential in the product analysis phase, which works especially well with micro-sized electrophoresis chips. Currently, micro-sized versions of classical electrophoresis chips become more and more prominent due to their low cost compared to conventional benchtop devices [205].

The design of electrophoresis systems is rather simple and consists of the elements: (i) injection zone, (ii) separation channel, (iii) detection zone as shown in Fig. 4. Due to the advancement of micro and nanofabrication techniques, it is possible to integrate the electrophoresis system with functional elements like a mixture or a reactor. This enables real-time analysis, which helps in the realisation of micro total analysis system ( $\mu$ -TAS) or lab-on-chip, achieving improved efficiency.

Typical channel dimensions vary from 10-300 µm in width and 5 - 100 µm in depth. Abrasive jet machining is the most widely used method apart from the utilisation of dicing blades to produce microchannels on the substrate. In abrasive blasting method, high etching rates up to 100 µm/min were achieved [202]. The substrate containing the microchannels is attached to flat glass or silicon substrate to form a closed enclosure. Abrasive jet machining and abrasive blasting are commonly used to create an inlet, outlet, and electrode opening on these materials. Additionally, the abrasive blasting method is used to improve the surface finish of the separation channels [20]. It was reported that it is possible to achieve a separation channel's surface finish ( $R_a$ ) as low as 0.1 µm with 5 µm sized abrasive particles in the abrasive blasting method. However, the small size abrasive particles non-reusability leads to higher processing costs [259].

### 2.1.2 Micro pumps

Microfluidics has provided attractive solutions for pharmaceutical fields like drug delivery. Irrespective of the field of application, precise dosing and transportation of small volumes of fluid to the targeted area is frequently needed, and for this purpose, micro pumps have been developed with different actuation mechanisms such as magnetic [208], electromagnetic [264-267], and ferrofluid based magnetic actuation [262,263] (Fig. 5).

### 2.1.3 Micro mixer

In general, microfluidic devices consist of a microchannel network for transporting fluids to regions. Usually, the dimensions of the channels are in the range of 10- 100 µm, which results in low

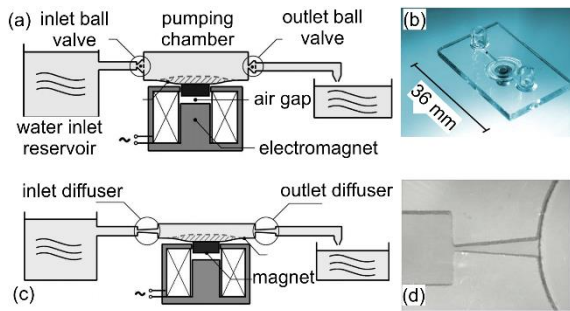


**Fig. 5.** Schematic diagram of (a) a ball valve micro pump (b) an example of an assembled ball valve micro pump (c) a diffuser micro pump with external electromagnetic actuation (d) a close view of an inlet diffuser produced on a glass substrate (manufacturing method: abrasive blasting) [264,265].

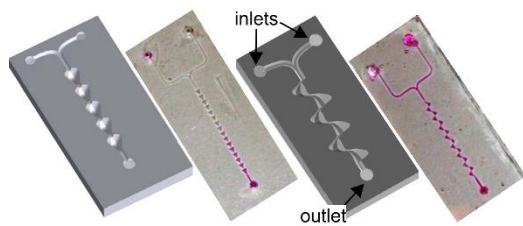


**Fig. 6.** Schematic view and actual representation of micro mixers with different 3D microstructures (manufacturing method: abrasive blasting) [203].

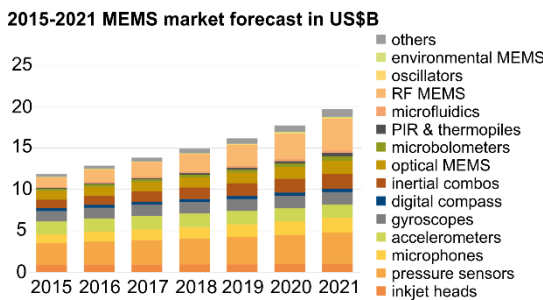


**Fig. 7.** MEMS market forecast [104].

Reynolds numbers ( $Re \sim 1$ ) making the flow laminar. In the applications mentioned in section 2.1.1 and 2.1.2, it is advantageous. However, it can pose a problem in applications where mixing of different fluids is required as it takes much time under laminar flow conditions. To overcome such limitations, solutions were proposed to generate 3D microfluidic structures with complex geometries to promote turbulent mixing. Researchers have demonstrated abrasive blasting as a single step method for manufacturing micro mixers to be economical by avoiding conventional technologies like photolithography and etching, which consists of several manufacturing steps (Fig. 6) [203]. Moreover, abrasive blasting was also used for finishing the 3D microstructure surfaces, which enhances the fluid flow. For mixer devices, glass is still a preferred material over polymers such as Polydimethylsiloxane (PDMS) and PMMA due to its chemical and electrical resistance [200,203].

## 2.2 Micro electro mechanical systems (MEMS)

Another promising application of abrasive micromachining is the manufacturing of MEMS. These are sensors and actuators with a typical feature size between 1-100  $\mu\text{m}$ . The advantages of making such small devices are fast response time, low weight, small volume and the utilization of micro-scale effects, such as: gravity

becomes negligible compared to adhesive and friction effects, surface tension dominates gravity, etc. Examples of commercially successful MEMS are inkjet nozzles, airbag sensors and pressure transducers [246]. Fig. 7 shows the worldwide MEMS market revenue breakdown in 2015 and forecasted market up to 2021.

### 2.2.1 Sensory devices

During recent years, erosion based abrasive blasting technology has been widely used to produce various sensor devices as shown in Fig. 8. Traditionally, micro-structuring for sensor applications is realized using aggressive hydrofluoric acid-based wet etching method, limited to produce microstructures with isotropic profiles. In contrast, the abrasive blasting technique enables complex and controlled shapes of the eroded structures. Moreover, the erosion rate of the abrasive blasting process is typically several hundreds of micrometers per minute, which is much higher than standard wet or dry etching processes' removal rates [22]. This makes the abrasive blasting technology very appropriate for fast and complex three-dimensional micro-structuring without any upper limits in the part size. [192] used a high-speed table reversal mechanism in grinding process (very high feed rates at high stroke rates) to produce micro slots with an aspect ratio 15 in hard, brittle materials like tungsten carbide and alumina for sensor applications.

### 2.2.2 Piezoelectric transducers

Piezoelectric thin films are useful in applications that require low power and low noise, high frequency and large output signals. Piezoelectric thin films application includes MEMS actuators, resonators, and filters [271], a broad range of lab-on-a-chip applications such as biosensing, particle/cell concentrating, sorting/patterning, pumping, mixing, nebulization and jetting [77]. Among many other piezoelectric materials, AlN, ZnO, and Pb ( $\text{Zr}_{1-x}\text{Ti}_x$ )  $\text{O}_3$  (PZT) are most widely used. The abrasive processes such as abrasive blasting and ultrasonic machining are used to produce pillars on these piezoelectric materials as shown in Fig. 9. Contrarily to dicing, abrasive blasting and ultrasonic machining allow to produce complex non-regular patterns.

## 2.3 Optics

Freeform optics is the next-generation of modern optics, exhibiting advantages of excellent optical performance and system integration. It finds wide applications in various fields, such as energy, illumination, aerospace and biomedical engineering. These freeform surfaces can be categorized as (i) continuous smooth surfaces (ii) discontinuous surfaces including steps or facets (e.g. Fresnel lens) (iii) structured surfaces, which are the arrays of structures for a specific function (e.g. surfaces with ridges) (iv) multiple surfaces on a single substrate [69]. The process chain for manufacturing freeform optics includes design, machining, moulding, metrology and evaluation. Moulding is one of the main processes for mass production.

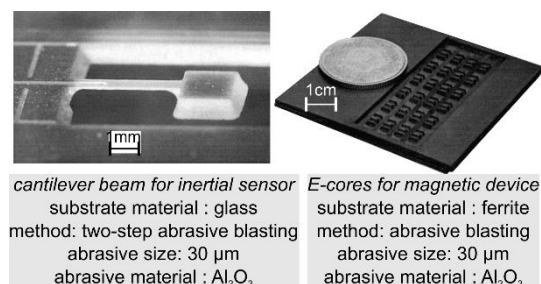


**Fig. 8.** Example of devices manufactured by abrasive blasting [22].

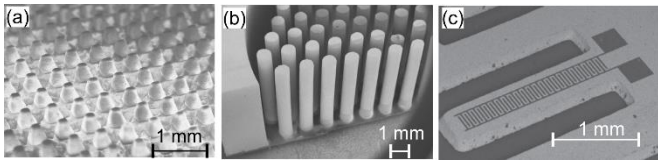


**Fig. 9.** Example of microstructures manufactured by (a) abrasive blasting (30  $\mu\text{m}$  size) and ultra-sonic machining (<1  $\mu\text{m}$  size diamond) (b) ultra-sonic machining (c) abrasive blasting on PZT material [23,29,166].

### 2.3.1 Moulds for producing micro lenses

The ability of abrasive processes to machine hard and brittle materials makes them suitable to apply them in optical applications such as finishing of moulding dies for lenses. In [220] e.g. grinding was applied to finish the tungsten carbide die for moulding of glass to produce Fresnel lenses as shown in Fig. 10. These micro-optical lenses produced via the ground moulds find applications in digital cameras, surveillance devices, endoscopy tools, blue-ray players and Fresnel lenses for solar panels.

In [268] a grinding method to manufacture moulding tools for manufacturing micro lenses with aspherical surfaces was presented. The authors were able to manufacture a moulding tool with a diameter of 3 mm [268].

A micro-grinding process with 10-20  $\mu\text{m}$  sized diamond bronze bond tools was used for rough cut and 2-4  $\mu\text{m}$  diamond resin bond tools for finishing aspheric optical surfaces in glass [75]. They achieved a surface roughness of 100  $\text{\AA}$  RMS, and less than 1  $\mu\text{m}$  of sub-surface damage/cracks in 30 min (workpiece size: 40-50 mm in diameter, 120 mm convex radius of curvature). The authors were able to finish different kinds of materials such as optical glass, ZnSe,  $\text{CaF}_2$ , ZnS, and silicon. Some researchers have applied vibration assisted polishing (with 0.5  $\mu\text{m}$  diamond slurry) to finish the die surface for producing micro-optical lenses and were able to achieve less than 5 nm surface roughness ( $R_z$ ) [92,219,221].

### 2.3.2 Optical waveguides

Another primary application of abrasive process can be found in the manufacturing of optical waveguides on Lithium niobate. Optical waveguides are basic photonic components which confine the light propagation in very small volumes with dimensions of micron or sub-micrometer scales. The light inside the guiding structures could reach relatively high optical intensities compared to the bulk geometries without waveguides.  $\text{LiNbO}_3$  integrated optical devices require micro sized structures such as ridge guides, Bragg gratings and photonic crystal structures.  $\text{LiNbO}_3$  substrates with ridge waveguides have attracted much attention over the past thirty years because they constitute the base of many optoelectronic devices in integrated optics (e.g., optical switches, modulators, couplers, multiplexers, etc.). There are many methods for the manufacturing of  $\text{LiNbO}_3$  ridge waveguides, such as dicing, femtosecond laser ablation, ion beam etching, plasma etching, and

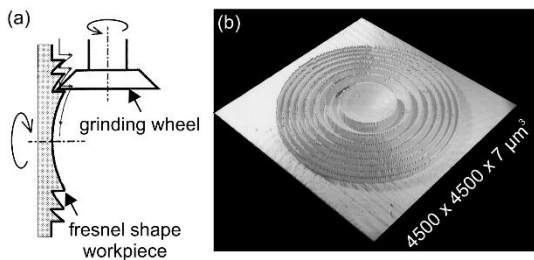


**Fig. 10.** (a) schematic of grinding process to produce die surfaces for Fresnel lenses moulding (b) 3D view of tungsten carbide die for Fresnel surface moulding [220].

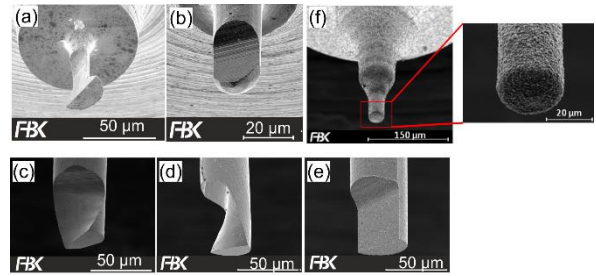


**Fig. 11.** Micro end mill with (a) dovetail shape (b) ball end, with a helix angle of (c)  $-30^\circ$ , (d)  $0^\circ$ , (e)  $+30^\circ$  manufactured with thin grinding wheels [11], (f) micro pencil grinding tools manufactured with thin grinding wheels [Source: FBK, TU Kaiserslautern].

sputter etching. However, precise diamond blade dicing is a useful technique for manufacturing ridge waveguide structures because dicing integrates both cutting and polishing [279]. Moreover, with dicing blades, it is also possible to produce high aspect ratio structures (>500) (Fig 4b), which reduces the propagation losses as low as 0.5  $\text{dB cm}^{-1}$  [56]. Ridge waveguides on Nd: CNGG crystal were also produced applying diamond dicing blades [147].

### 2.4 Manufacturing of cutting tools

Another famous category of products are micro tools themselves. Several researchers have reported the development of micro tools such as micro end mills or micro pencil grinding tools applying manufacturing processes like grinding, electrolytic in-process dressing (ELID) grinding and processes assisted with abrasives such as wire electric discharge grinding (WEDG).

#### 2.4.1 Micro tools production

In [10,11] the manufacturing of micro end mills and micro pencil grinding tools with thin diamond grinding wheels was demonstrated. As it is essential to control the process forces during the manufacturing of micro tools, it was recommended to use small grain sizes and a thin grinding wheel. It was also mentioned that manufacturing of micro tools using grinding results into short machining times. For example, the grinding time is less than 10 min for manufacturing micro-end mills with diameters from 10 to 50  $\mu\text{m}$ . The same research group has demonstrated the capabilities of grinding to produce different geometries of micro end mills as shown in Fig. 11.

In [178] super fine abrasive wheels in ELID grinding were used to manufacture tungsten carbide micro tools with a variety of shapes. They were able to produce cylindrical tools with less than 1  $\mu\text{m}$  tip diameter as shown in Fig. 12.

The inclusion of ultrasonic vibrations during the grinding process enables to produce 50% higher aspect ratio and 10 – 20% smaller diameter micro tools compared to the grinding process without ultrasonic vibrations [182].

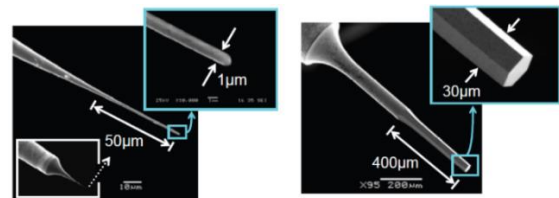


**Fig. 12.** Overview of micro tools produced via ELID grinding [178].

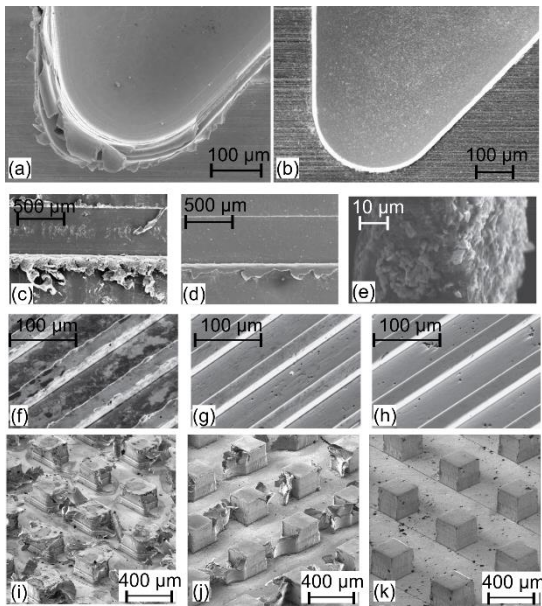


**Fig. 13.** SEM-views of the edge of a micro milled cavity before (a) and after (b); deburring by ultrasonic wet peening of a micro milled copper surface (c) before deburring (d) after deburring; (e) SEM image of a nylon bristle embedded with 3 μm SiC abrasive abrasive grits; brass mold surface (f) before deburring (g) after deburring process for 4 min (h) after deburring process for 10 min; micro milled pillars on aluminum alloy (i) before deburring (j) after polishing (k) after abrasive waterjet machining on polished surface [103,112,156,159].

#### 2.4.2 Coating Pre-/Post treatment

In [225] a micro-abrasive blasting process was applied on tungsten carbide surface as pre-treatment process to enhance the adhesion strength of the sputtered coating. The main reason for this phenomenon can be attributed to the resulting high compressive stresses on the substrate surface [224]. A similar approach was adopted to enhance the coating strength of different cutting tools [27] and to improve tool life [28,122]. This micro blasting process also removes subsurface damages resulting from the macro grinding process. Hence, it was used as a post-treatment process for ground surfaces [225,226].

#### 2.5 Deburring via micro-abrasive processes

Burrs in micro parts need to be removed for the proper functioning of the parts. The abrasive assisted deburring process presents a fast and effective method for deburring these parts. One such process is micro abrasive peening. Micro-abrasive peening was used to deburr, smoothen and to remove the texture marks on the micro-milled X38CrMoV5-1 VMR [103].

Several investigations were made on abrasive assisted brush deburring processes. A nylon bristle brush with embedded abrasives was used to remove burrs of a micro-milled surface [156,157]. A method was proposed for deburring micro moulds with a magnetorheological fluid consisting of 2 μm sized diamond abrasives. Metal burrs with a height of 200 μm and thickness of 1 μm were removed successfully [112].

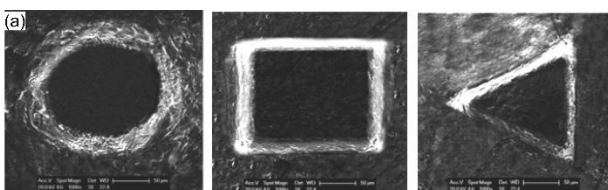


**Fig. 14.** SEM images of single abrasives [12].

A two-step polishing and abrasive waterjet machining method was developed to remove burrs on micropillars [159]. In [185], a magnetic abrasive finishing process for deburring of electronic gun parts used in TV monitors was developed. All mentioned examples can be found in Fig. 13.

### 3. Micro Abrasive Processes

#### 3.1 Abrasives

The continual developments of High-Pressure High-Temperature (HPHT) catalyst based synthesis processes have resulted in the production of a wide range of synthetic diamond and cubic boron nitride abrasive materials, ranging from sub-micron to several millimetres [234]. Modification to the crystallographic structure of diamond and cubic boron nitride can also be achieved with HPHT synthesis. For instance, by the introduction of micro-diamond or cubic boron nitride crystal seeds into the synthesis ingredients and by controlled pressure/temperature parameter variations, multi-crystal growth orientations (twins) can be achieved to form polycrystalline diamond or cubic boron nitride crystal structures [76].

The products that are derived from these abrasives, typically consist of selected distributions of crystal shapes produced from selections of the as-synthesised crystals or from further processed (naturally occurring or synthesised) crystals which have been reduced in size through crushing or ball milling. These products are graded by their manufacturers with a friability strength or toughness index which denotes the resistance to fracture.

Conventional diamond or cubic boron nitride (cBN) layers, such as those used in micro-tools, generally consist of a monolayer (e.g. brazed or galvanic bonded) or multilayer (e.g. moulded, vitrified or sintered) of grains. These layers result in having a population of individual diamond or cBN abrasive grains with random crystallographic orientations, irregular inter-particulate spacing and protrusions from the bond surface. Such arrangements therefore result in significant differences in strength of the individual abrasives [251] due to the anisotropic nature of the abrasive material and to the differences in crystal shapes. In addition, their stochastic distribution results in irregular geometries, uneven loading and undefined chip/debris flow paths across the tool surface. Such limitations in traditional diamond and cBN abrasive surfaces have been addressed by research into novel processing methods to produce regular surfaces featuring abrasives with uniform characteristics, as described following.

##### 3.1.1 Micro-abrasive elements

In the case of conductive materials (e.g. PCD), EDM and crystal growth methods can be employed to generate ordered abrasive surfaces for grinding/polishing applications [228]. While edge definition of the micro-cutting edges obtained by EDM process from the solid diamond structure is nevertheless time consuming and undercut features and geometries are difficult to obtain. The pulsed laser ablation process offers the controlled removal of material by considering various laser energy inputs (wavelength, pulse energy) and process kinematics (beam speed, pulse frequency) depending upon the type and topography of the target

The employment of the designed scan paths results in the selected removal of material (e.g. diamond, cBN) to produce the required features and geometries. This capability has enabled the generation of controlled (micro) abrasive shapes using solid diamond structures (e.g. CVD diamond) as the base material. In the case of monocrystalline diamond, the crystallographic lattice orientation can be selected to achieve high strength (e.g. {100} plane in the <110> direction) cutting edges of laser ablated features. To take the advantage of fully customizing grit shapes

using laser ablation process, several studies have been undertaken to obtain the better understanding of how different grit shapes and their specific micro-cutting edges can influence the grinding process results at micro scale [12]. Shape controlled micro-abrasives (figure 14) have been used in single grit scratch tests with zero clearance angle on ductile (Cu) and brittle (sapphire) materials.

Grits orientated in feed direction to present a defined Number of Cutting Edges (NoCE) as follows: circular NoCE = 0, square NoCE = 2, triangle NoCE = 3. It was reported that for copper, an increase in the grit NoCE results in more localised material side flow and reduced plastic deformations. For sapphire, fracturing phenomena was the preponderant material removal mode when using square/triangularly shaped grits while significant plastic deformations were found for circular base frustum.

Further, efforts have been made to understand the work material response to multiple passes with identical grits, which enable to design an abrasive tool with identical grits of regular arrays. Arrays of circular, square, and triangular grits have been generated (Fig. 15a) in identically shaped groups on a monocrystalline CVD diamond [32]. These arrays have been mounted on a grinding wheel hub (diameter 140 mm, cutting speed 35 m.s<sup>-1</sup>) and overlapped scratches have been produced with incremental depths of 1, 2 and 3 μm on Cu and Al<sub>2</sub>O<sub>3</sub> materials (Fig. 15b).

Studies on the cutting mechanisms of single defined shaped abrasives and controlled groups of abrasives in ductile and brittle materials have provided an understanding about work surface response to abrasive surfaces having defined geometry, grits count, and identical protrusion [33]. The characteristics of such surfaces can be customized depending on the material to be ground. Abrasive tools can be further customised to present abrasive grits with specific edge geometries (e.g. rake angles and clearance angles) so that the tool is composed actually of micro-cutting edges [184]. Such a hybrid tool with the functionality of grinding but with the grits of identical geometry was developed as shown in Fig. 16.

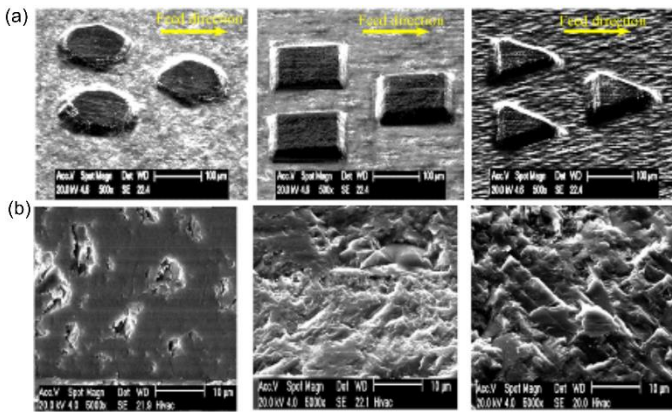


Fig. 15. (a) SEM images of shaped abrasive groups and (b) scratches produced by circular, square, and triangular shaped grits on sapphire [32].

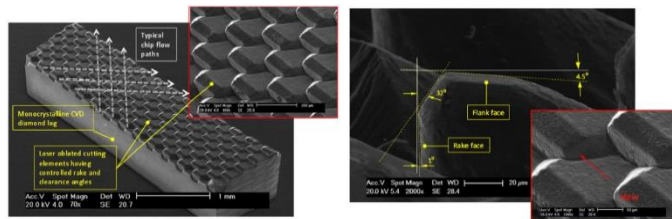


Fig. 16. Laser generated diamond micro abrasive arrays showing geometries and chip flow paths [34].

Substantial improvements in surface finish and flatness of the ground surfaces and tool wear resistance have been obtained compared to the results with a conventional electroplated abrasive tool having equivalent grit size and density [34]. The primary wear mechanisms for conventional (polycrystalline) abrasive grits are micro fracture, flattening and cracking, while only a small extent of micro fractures can be observed for engineered abrasive grits for the same operational time. This is likely due to the uniform spread of load on the engineered abrasives in combination with the compact wear resistant columnar structure of the CVD diamond used. These comparative wear studies open opportunities for the design of negative rake grinding tools for industrial applications [184]. SEM images supported by surface morphological investigations between the surface machining and planetary grinding process has enabled the understanding of the interaction mechanisms between conventional/engineered abrasive grits and workpiece surface, which allows to define the key design parameters of the engineered grinding pads [278].

### 3.2 Chip formation in ductile and brittle materials when abrasive machining

The chip formation in micro-abrasive processes of ductile materials is similar to that of conventional macro-scale abrasive processes. An abrasive must reach a certain uncut chip thickness before a chip is formed [116,149,151], the so-called grain cutting depth. Abrasives contacting the workpiece that do not reach this grain cutting depth to form a chip cause rubbing and ploughing, i.e. friction. In addition, all grains forming a chip also contribute to friction and do only rub and plough before they reach the grain-cutting depth. That is, an abrasive undergoes three phases: I - elastic deformation (rubbing), II - elastic and plastic deformation (ploughing) and III - chip formation (grain cutting depth reached) [95]. The grain cutting depth depends on many influencing factors, such as the process kinematics, the lubrication conditions, temperature and properties of the workpiece and the geometry of the abrasive.

The proportion of phase III decreases with decreasing uncut chip thicknesses, the proportion of ploughing rises [222]. Hence, the proportion of ploughing is dominating at small uncut chip thicknesses [222]. Higher proportions of rubbing and ploughing at small uncut chip thicknesses result into high specific energies. This correlation is known as the size effect in grinding [13].

In micro abrasive processes, uncut chip thicknesses are very small. The proportion of ploughing can hence be expected to be very high [187], as are the specific energies [169].

However, the application of micro abrasive processes is more interesting for brittle materials, as other micro processes to machine ductile materials (milling, ultra-precision turning) are more developed and achieve high process reliability [71]. The chip formation of brittle materials is nominally different than that of ductile materials. Brittle material removal at high chip thicknesses is governed by crack initiation and propagation. These cracks result into fatigue of the material and ultimately in the break-out or spalling of parts of the material [24]. This results into non-sharp edges, so-called chipping and notches on the surface. In addition, non-visible cracks in the workpiece that can result in the premature failure of the workpiece can exist [151,210].

With appropriate process conditions, brittle materials can be machined in a ductile manner. That is, flow-like chips can be produced [2,106,270], resulting in smooth or typical ground surfaces [171] and sharp edges of the workpiece [9]. This process regime of brittle materials is named ductile mode or ductile regime machining [24]. The mechanism of ductile regime machining or the processes within the material respectively are not fully understood to date. The knowledge of grinding in ductile mode is

based on the knowledge of tribology and material science, i.e. on scratch and wear tests on brittle materials. Most theories refer to the occurrence of high hydrostatic compressive pressures in the material that result in the ductile behaviour of brittle materials [68,151,204,270] going back to early material science theories of Mohr [167]. Those hydrostatic pressures reduce the tendency of crack initiation [25] or hamper those [150], as crack initiation only occurs at tensile stresses [5]. Hydrostatic compressive stress fields are intensified by negative shear angles [25,252,270], as present in abrasive processes. Another hypothesis of ductile regime machining is based on energetic considerations. This hypothesis is based on the assumption of a critical dimension of material removal at the single grain or the material removing indenter. Below this critical dimension plastic deformation prevails, as a brittle fracture or microcracks are inhibited [117,150,197] or the induced energy is not sufficient to initiate cracks respectively [24,130]. Other theories refer to always present cracks in brittle materials that are not increased when a critical dimension of material removal is maintained, or the fracture toughness of the material is not exceeded [141,229,233].

More recent works apply Molecular Modeling (MD) approaches to explain the mechanism of ductile regime machining for ultra-precision machining on the nanoscale. [36] were able to show that if the chip thickness is below a specific threshold value, compressive stress is induced into the material, hampering crack propagation and that at sufficiently low chip thicknesses the shear stress is higher than the yield stress and hence dislocation motion is possible [35]. In [223] it was also revealed that shearing under compressive stresses for silicon results into ductile regime machining. The simulations in [252] suggest that brittle fracture when exceeding a certain chip thickness can be led back to the initiation of tensile stresses.

Although the exact mechanisms of ductile regime machining of brittle materials are not fully understood, numerous empirical examinations prove its existence. In [197] scratch tests demonstrated that a ductile material behaviour exists when a certain threshold of forces is not exceeded. The force component in the normal direction, towards the finished surface is decisive [62]. A ductile mode prevails, when the resulting load of a single grain is below a material-specific threshold value [124], i.e. the load per grain has to be low [183]. As the load per grain is directly linked to the chip thickness, the chip thickness is used as the characterizing value for the transition of brittle to ductile material behaviour.

According to [24], a material-specific critical chip thickness  $h_{cu, crit}$  is not to be exceeded. This model is based on indentation tests [130], where a critical indentation depth based on the module of elasticity, the hardness and the criteria of propagation of cracks was defined. The criteria of propagation of cracks again were found to be proportional to the ratio of hardness and fracture toughness  $K_c$  [155]. The critical indentation size  $a_c$  was found to be proportional to material properties [155].

$$a_c \sim \left(\frac{E}{H}\right) \left(\frac{K_c}{H}\right)^2 \quad (1)$$

where  $E$  is the Modulus of Elasticity,  $H$  is the hardness of the Material and  $K_c$  is the fracture toughness

For brittle materials, the term  $E/H$  is in a close range. Hence the term  $K_c/H$  defines the differing behaviour of different materials [26]. This term is also called brittleness index. It has to be noted that the Hardness  $H$  is load-dependent. To quantify the critical chip thickness, experiments were conducted in a large variety of brittle materials. The empirical values of the depth of cut with a very stiff high precision grinding machine were compared to the critical indentation depth and a correction factor of 0.15 was found for the proportionality equation from [155] the critical chip thickness defined as (24)

$$h_{cu, crit} = 0.15 \left(\frac{E}{H}\right) \left(\frac{K_c}{H}\right)^2 \quad (2)$$

He found that this correction factor is valid for a wide range of materials. However, it has to be mentioned that the correction factor depends on several factors, not only the material but also the machine tool, the grinding wheel specifications and the kinematics [145]. Numerous authors examined the critical chip thickness and found that it is in the range of 0.01 to a maximum of 2  $\mu\text{m}$  [4,14,140,145,162,170,204,242,249,280]. A frequently used value is 1  $\mu\text{m}$ . Due to the very low uncut chip thickness in micro abrasive processes, such chip thicknesses are easy to achieve, as shown in recent works (see following subsections).

However, actual research reveals that a simple downsizing of macro grinding is not possible. There is some evidence that the critical chip thickness in micro grinding is smaller than in macro grinding. In [48, 51], ductile mode regions were defined based on crack length measurements on the workpiece. For silicon, they defined ductile mode cutting for undeformed chip thicknesses smaller than 20 nm, followed by a ductile-brittle transition area, while a brittle mode is reached with undeformed chip thicknesses bigger than 100 nm. For soda lime glass the values were even smaller, with the ductile mode at undeformed chip thicknesses smaller 2 nm and brittle mode at undeformed chip thicknesses bigger 5 nm. Those values are much smaller than those reported for macro grinding. Other experimental works also confirm this [40]. The transition to a ductile mode for silicon was found at around 20 nm uncut chip thickness.

Both researchers compared the experimentally observable transition areas with analytical calculations of the chip thickness. This entails simplifications that could result in the deviations between the values of the critical chip thickness for macro and micro grinding. Models and knowledge about chip formation in micro abrasive processes are not fully explored, and most references on chip formation are derived from macroscale abrasive machining. Single grain scratches, as applied to understand chip formation in grinding, can hardly be downscaled to process conditions of micro abrasive processes. Newer works focus on modelling micro abrasive processes, applying known relationships of macro abrasive processes [50,187,207], see also section 4.

### 3.3. Micro Grinding

Micro grinding includes all techniques to produce microstructures using bond abrasives. Among the widespread dicing, wire cutting and Micro Pencil Grinding Tools, also engineered macro grinding wheels to produce microstructures as well as Electrolytic in-process dressing grinding will be briefly presented.

#### 3.3.1. Dicing Blades and wire cutting

Fine cutting using dicing blades or abrasive wire cutting is nowadays extensively employed for slicing electronic materials (e.g. silicon wafers) which are subjected to tight surface quality requirements (surface roughness, cut straightness, chipping/fracture edge avoidance). With thickness varying from tens to hundreds of microns, the dicing blades are commonly made of diamond abrasives (avg. grit size 5-20  $\mu\text{m}$ ) in various matrixes (e.g. Ni, glass, etc).

In [237] a literature review of the wire sawing technology is given in which both multi-wire slurry and diamond wire sawing, different ingot materials, modeling of grit indentation and sawing process were included and reviewed. The development of fixed abrasive diamond wire machining and the advantages were presented and introduced in [55]. The cutting mechanism including wire bow, cutting force and wire tension force was presented in detail.

Dicing blades were fabricated and their cutting performance compared with commercial blades. It was found that the fabricated blade which was made of a vitric material with pores had the better cutting ability because of the flesh diamonds, created by wear during cutting, on the surface [158].

Scratching tests were carried out on silicon wafers and it was concluded that the chipping modes could be categorized into four types in different angles (Fig. 17) and that the chipping modes were dependent on the cutting direction and slip direction of the wafer [148]. It was concluded that the blade surface condition is an important factor to affect chip sizes and that the chipping size is big at the first cutting stage (cutting distance of 0-300 m) while it decreased at steady stage (300-2000 m) [139].

Multiple micro profiled metal bonded diamond grinding wheels are used to machine microstructures in brittle-hard materials to improve the productivity and get high geometric accuracy because of the higher tool stiffness, low wear and high profile retention [59]. [135,276] studied material interaction during micro-grinding, one on Reaction-Bonded SiC/Si composite (Fig. 18) and the other on maraging steel. A technique was developed to fabricate an extremely thin diamond micro wheel with the micro co-deposition method and the tool was used to implement microgrooves on optical glass in situ (Fig. 19). It was concluded that the developed tool could generate a better accuracy and good geometry in micro-grooving [46]. Another similar method was proposed to carry out precision dicing on hard and brittle materials while the metal-bonded blades are laser-dressed in situ [250]. To improve machinability, in [132] a method was developed to produce dicing blades with photopolymerizable resins, and the working performance was investigated via testing of different kinds of designed blades while an ultrathin dicing could be obtained using a spin-coating process.

Work performance of electroplated diamond wire saw is investigated with a different combination of wire speed and ingot feed speed when slicing single crystal silicon [80]. It was indicated that the introducing of cutting fluid would give better wafer quality and the wire wear mainly came from pulled-out diamond abrasives (Fig. 20).

In [244] slicing solar silicon ingot using an abrasive electrochemical method with the help from a multi-wire saw system was proposed and the corresponding manufactured product was investigated. It showed that this method occupied the advantages of a higher production rate, low cost and better-machined surface integrity.

In [57] a performance comparison of ultra-precision dicing and wire sawing in machining two silicon carbide variants materials was carried out. It was concluded that both techniques could carry the task, but dicing showed advantages on edge chipping and sidewall roughness while the wire sawing gives lower sidewall curvature.

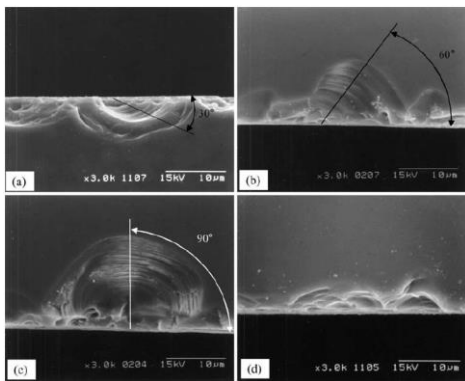


Fig. 17. Different chipping on the die edges during the dicing silicon wafer. a)30°, b)60°, c)90°, d)irregular [148].

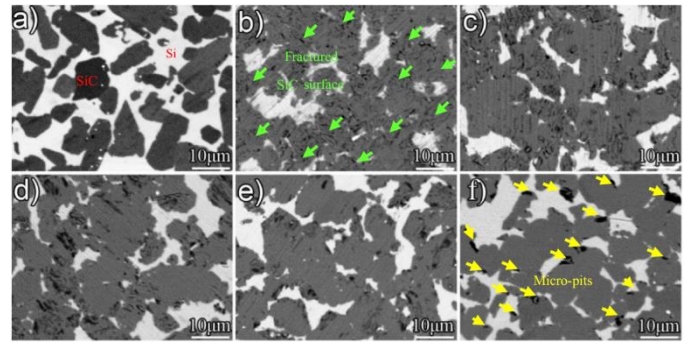


Fig. 18. SEM surface morphology at different feed rates. [276].

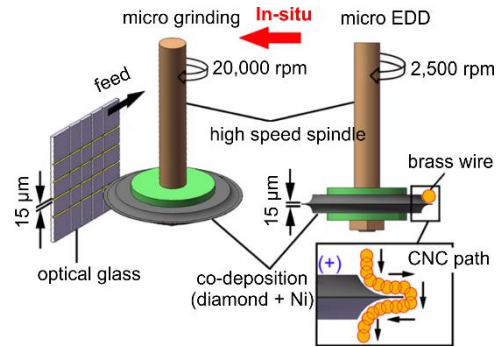


Fig. 19. In situ approach for micro grooves [46].

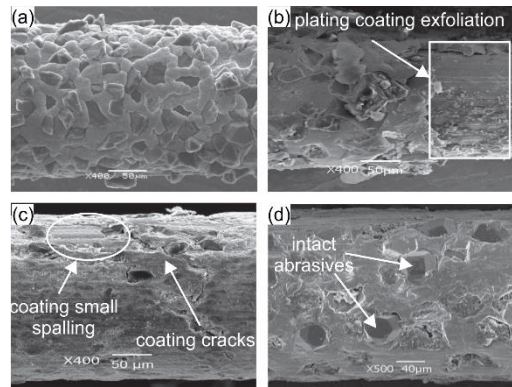


Fig. 20. SEM pictures of diamond wire at different wear conditions [80].

### 3.3.2. Micro Pencil Grinding Tools

Micro pencil grinding tools (MPGTs) (also called micro grinding tools, micro-abrasive pencils, micro-abrasive tools, abrasive pins) consist of abrasive grits that are bonded to a base body. These MPGTs are used to produce microstructures of various sizes and shapes on hard and brittle materials (Fig. 21).

Specifically, these micro tools are used to produce and finish microfluidic devices, moulding or extrusion tools, microreactors, separators of micro fuel cells, precision components like nozzles, microstructured surfaces and special products of precision engineering etc., and the cost may be competitive with other micro manufacturing processes [102,186].

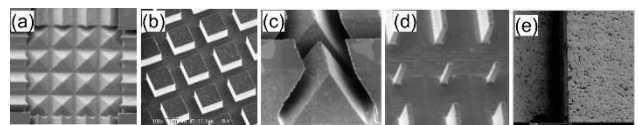


Fig. 21. SEM micrograph of microstructures produced on (a, b) silicon (c) glass (d) zirconium oxide (e) tungsten carbide [Source: (a, c, d) [102] (b) [186] (e) FBK, TU Kaiserslautern].



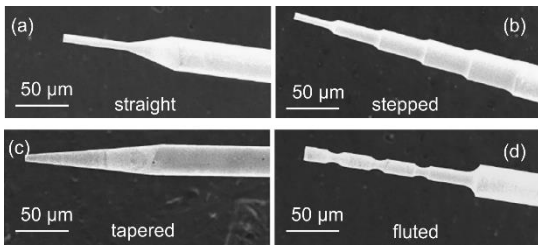


Fig. 22. Different shapes of tool substrates after  $\mu$ EDM process [47].

There are mainly two steps involved in the manufacturing of MPGTs: the preparation of the base substrate geometry and the deposition or coating of abrasive grits to this base substrate, forming the abrasive layer. The layer design differs mainly concerning the grain size and their deposition method on the base substrate. The sizes of MPGTs ranges from few millimetres down to 4  $\mu$ m [9]. Dicing blades or thin grinding wheels are widely used to generate the geometry of the initial tool blank due to the high achievable material removal rates compared to other processes like EDM, WEDM, and WEDG. However, all these processes have the flexibility to manufacture the tools in different shapes like those shown in Fig. 22.

Cemented carbide consisting of tungsten carbide in a cobalt matrix is the commonly employed base substrate due to its high bending strength and stiffness compared to other possible material such as steel. This material also allows the manufacturing of micro tools with very low diameters and high aspect ratios [10]. Abrasive grits can be coated or deposited on the base substrate by vapour deposition or embedding techniques such as:

- electroless plating [7,8,186]
- electroplating [9,131,181]
- micro machining of sintered PCD blanks [37,72-74]
- sintering [41,245,269]
- electroforming [47]
- HPHT synthesis (boron doping) [45]
- CVD [78,79,101]
- cold spraying [89]

It can be deduced that electrolytic (electroplating and electroless plating) techniques are most widely used to produce MPGTs; this is due to the low manufacturing costs and reduced processing time [186].

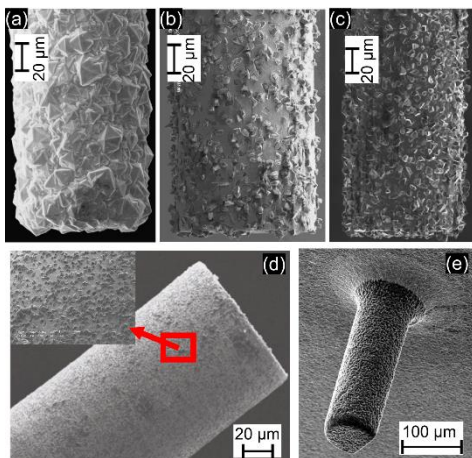


Fig. 23. Comparison between MPGTs topographies produced with different methods (a) CVD [78], (b) electroplating [181], (c) electroless plating [186], (d) cold-spray [89] (e) sintering [168].

However, according to [79], the CVD coating method is economical despite prolonged coating times for large batch production as thousands of tools could be coated in one process in bigger reactors. As mentioned above, some researchers have considered macro-sized sintered PCD blanks, where their size was reduced to the micro level with  $\mu$ EDM or WEDG process. The base substrate of sintered PCD tools also consists of diamond grits; during the  $\mu$ EDM or WEDG process, the diamonds are exposed. Fig. 23 gives a comparison between the topography of micro-grinding tools prepared with different methods.

A comparison between the different embedding/coating methods is given below (Table 1) concerning MPGTs requirements for the micro-grinding process.

Table 1. Comparison of different coating methods [41,78,79].

	EP	ELP	CVD	importance
process time	↓	↓	↑	low
processing cost	↓	↓	↑	low
process temperature	↓	↓	↑	low
tool life	↑	↑	→	high
chip space	↑	↑	↓	high
layer thickness	↑	→	↓	high
adhesion to the base substrate	↓	→	↑	high
coating uniformity	→	→	↑	high
EP – electroplating, ELP – electroless plating high ↑, medium →, low ↓				

For all coating methods, the challenge is to select the appropriate coating parameters to achieve the required coating thickness at high uniformity. There are several parameters which can affect these responses. In an electroless plating process, for example, thiourea concentration, grit concentration, substrate rotational speed, and embedding time etc., [9]. Several studies found in literature contribute to a better comprehension of the coating process. However, applying univariate methods in their works cannot allow the evaluation of simultaneous effects of more than one deposition parameter on the same response.

### Application of MPGTs

The micro-grinding process chain consists of several steps: substrate preparation, coating of substrate and micro-grinding itself. According to these steps, the available studies can be classified in three types:

- (i) Investigations to understand the micro-grinding process mechanisms
- (ii) Investigations to improve the quality of the tools and the process
- (iii) Investigation of tools for hybrid processes

### Investigations to understand the micro-grinding process mechanisms

One of the key advantages of the grinding process compared to other machining processes is its capability to machine hard [10,79] and brittle materials (silicon [37,45,49,51], glass [72,73], alumina [74], zirconia [101]). However, few ductile materials [7,89,131,137,181] are also examined.

The quality of the parts produced is influenced by the process conditions, micro-grinding wheel properties, and microstructure of the materials to be machined or structured. In spite of the complexities associated with the tool manufacturing and their unpredictable nature, significant efforts have been made to understand micro-grinding of ductile and brittle materials.

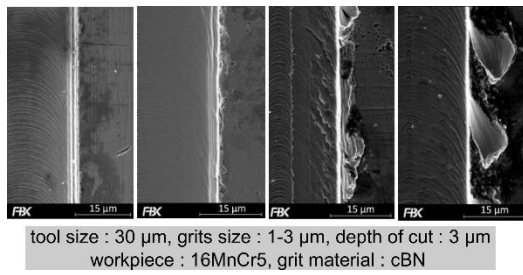


**Fig. 24.** Burr formation in AISI 4140H with different feed rates (left to right: 0.1, 0.3, 0.6, 0.9 mm/min) [237].

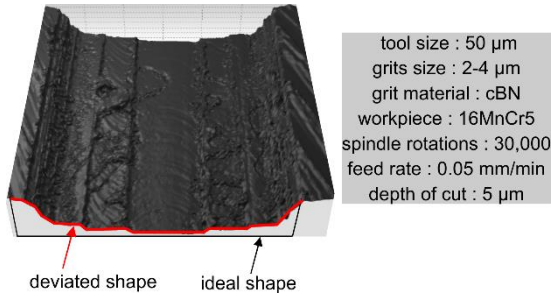


**Fig. 25.** Geometrically deviated step-shaped structure resulting from the micro-grinding process [206].

Burr formation in micro-grinding of ductile materials is a common issue. The burr forms along machined microchannels as shown in Fig. 24 and its size is increased with increasing feed rates. Due to the difficulties associated with deburring of micro scaled structures, avoiding burrs is a primary goal of micro-grinding process developments. To achieve this, it is essential to obtain the optimum grinding conditions considering minimum chip thickness values and process kinematics.

In micro-grinding of brittle materials, workpiece fracturing is a concern. Several experiments were conducted to investigate the ductile-brittle transition (compare section 3.2) [48–50,72,73]. To monitor these transitions, the dynamic forces during micro-grinding process were considered [49]. Forces in the ductile mode of cutting region are stable whereas in the brittle region they are unstable with large fluctuations as shown in Fig. 40. With this approach, the process can be monitored and controlled to achieve a high machining quality. In another approach, a method was proposed where a resin coat is implemented on the top of the workpiece to minimize micro fractures [51].

In micro-grinding processes, it is common to conduct the experiments with low depths of cut compared to the grit size to overcome the risk of premature tool failure (Table 2). In doing so, only few grits located on the tool bottom surface participate in the cutting process. This results in geometrically deviated structures as depicted in Fig. 25.

**Table 2.** Summary of experimented grit size and depth of cut comparison.

end diameter (μm)	depth of cut per pass (μm)	average grit size (μm)	reference
50	10	7.5	[7]
70	10	10	[37]
600	20, 50	30	[49,50]
850	3	63	[74]
850	2,4,6	63	[72]
850	3,5,7	101	[73]
1000	3, 5	50	[79]
1500	15, 30	108	[131]
1000	5, 15	56	[131]
600	50	76	[137]

The clogging is most intense at the tool bottom. Some researchers attempted to optimize or modify the tool bottom surface geometry by μEDM and dressing [72,74,245]. [237] utilized a μEDM process to create a cavity inside the tool substrate. Machining results proved that this modification improved the results in terms of clogging as well as eliminating the aforementioned step at the channel center position as shown in Fig. 27c - Fig. 27d.

To understand the correlation of the tool topography and the deviation of structures, a kinematic simulation of the micro-grinding process was performed [206]. The results revealed the influence of the maximum protruded grit's radial positions on the tool bottom surface on the geometrical deviations. Besides, it was shown that a high number of grits towards the outer surface of the tool results into the minimization of these deviations. Hence, any effort towards minimizing the number of grits at the central region on tool bottom surface will enhance the micro-grinding process efficiency. Such approaches are discussed in the following subsection.

#### Investigations to improve the quality of the tools and the process

When micro-grinding, premature tool breakage is very common due to its high aspect ratio. To prevent this, [37,45] adopted a tangential force feedback mechanism to control the feed rate intermittently. Besides, micro-grinding tools are prone to high tool wear due to the high amount of rubbing and ploughing and hence friction in the process. To minimize this, several researchers used different cooling strategies. Among those are chilled air and minimum quantity lubrication. [6] applied water based sodium dodecyl sulfate (SDS) fluid in MQL mode, and achieved prolonged tool life, less burr formation and minimized adhesion of chips to the work surface. [131] reported that the electroplated cBN grinding tool (case 1) could absorb much more heat generated at the tool-workpiece contact interface than the vitrified cBN grinding tool (case 2). As a result, applying compressed air for cooling, lower grinding forces were achieved in case 1.

Clogging is a severe issue in micro-grinding. While in conventional grinding this issue is known from very ductile materials like Aluminium, in micro grinding clogging of tools was also observed when grinding materials like case-hardened 16MnCr5 (665 HV30 ± 15 HV 30, AISI 5120) (Fig. 26).

Adhesion and clogging of chips to the tool surface leads to a rise in temperature, forces and ultimately coating failure. To avoid this, the tool surface must have enough chip space. The lack of chip space is also one of the main reasons that limits the use of CVD coated tools despite their excellent coating adhesion to the base substrate. This effect can be minimized through the proper application of coolant [6] and via ultra-sonic assisted grinding [181]. According to the authors, the application of ultra-sonic vibrations resulted in considerably reduced clogging. However, grits on the wheel end face and edge were almost crashed.

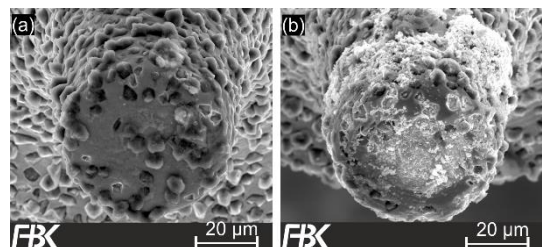


**Fig. 26.** Effect of clogging on MPGT (a) before grinding (b) after grinding [7].

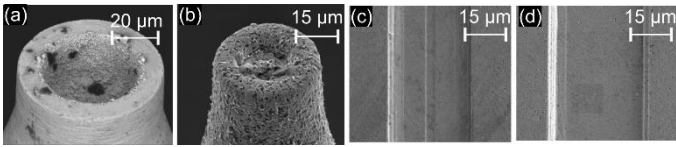


**Fig. 27.** (a)  $\mu$ EDM machined tungsten carbide blank (b) electroplated micro pencil grinding tool (c) grooves produced on tungsten carbide surface with unmodified tool (d) grooves produced on tungsten carbide surface with the modified tool [source: (a, b) [236], (c, d) [237]].

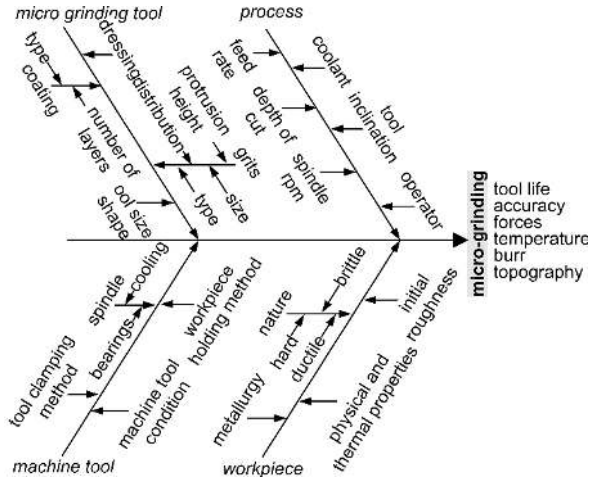


**Fig. 28.** Cause and effect diagrams for micro-grinding processes.

### Investigation of tools for hybrid processes

Some researchers have applied micro grinding tools in combination with other processes such as EDM, micro milling, ECM and micro drilling. The tools which can be used to perform both processes are called hybrid tools, and the combined processes hybrid processes [37]. Based on the available findings, a cause-effect diagram has been designed to show the influencing parameters on the micro-grinding results (Fig. 28).

In spite of the micro-grinding process capability to machine hard and brittle materials, tools with high aspect ratio limit the feed rates and hence the achievable material removal rates. Another aspect that distinguishes micro from macro grinding is the influence of the grit distribution. While in macro grinding, due to the low sizes of the grits in relation to the tools, there is no visible or detectable influence of single grains on the workpiece quality, in micro grinding single grains can have a high impact on the workpiece surface.

### 3.3.3. Micro grinding with engineered grinding wheels

As outlined in chapter 2, microstructures can enhance the performance, lifetime and reliability of products. Besides micro abrasive processes with tools in the dimension of the structures themselves, there are also some examples where special macro grinding tools with dimensions of up to 400 mm in diameter were applied to produce microstructures. This is achieved by specially preparing or dressing the macro grinding wheels.

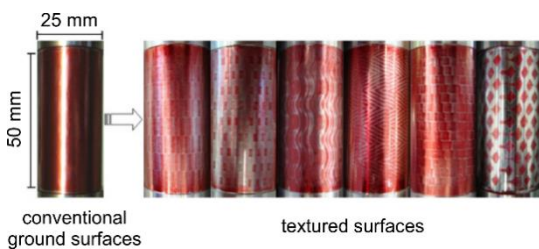


**Fig. 29.** Conventional and textured workpiece surfaces [180].

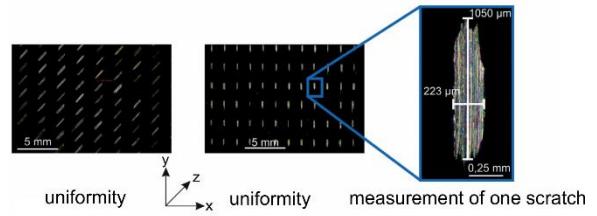


**Fig. 30.** Patterns produced in different orientations on flat workpieces using defined grain patterned wheel [212].

A dressing technique based on Acoustic-Emission mapping and control was used to inscribe pre-defined patterns or textures on the surface of conventional grinding wheels [180,213]. By choosing integer values of the speed ratio of the grinding wheel and the workpiece in cylindrical plunge grinding, the patterns of the grinding wheel were transferred to the workpiece surface (Fig. 29). This allowed for an increased tribological performance of the structured workpieces. In [212] a special cBN grinding wheel was presented (Fig. 38). The single grits were arranged in a defined gran pattern und dressed to a uniform grit protrusion. With such a grinding wheel with defined grain pattern, deterministic structured can be produced in flat workpieces at high speed and efficiency. Values of the specific cutting energy  $e_c$  reached values down to  $5 \text{ J/mm}^3$  [120].

Other works were concerned with mirroring the profile of precisely dressed grinding wheels into the workpiece. E.g. to produce riblets structures in workpieces [61], see Fig. 31. Such structures can decrease friction losses in gas turbines up to 10 %. More complex structures in surface were achieved by dressed, helical grooved grinding wheels in [217](Fig. 32). In [46] a method to develop an extremely thin diamond-grinding wheel was presented and to fabricate crisscross microgrooves on optical glass was presented Micro wire-EDM was employed for truing and dressing process. In [254] microstructures were produced on a non-coated cutting insert with 7–149  $\mu\text{m}$  in depth and 0.14–0.50 in aspect ratio on the tool rake surface with V-shaped grinding wheels. It was reported that these micro-grooved patterned tools decreases chip frictions and minimizes heat generation. Cutting temperatures were reduced by  $103^\circ\text{K}$  applying the structured inserts. The same approach was used to produce microstructures on a ball end mill [253].

Those approaches to use macro grinding wheels to produce microstructures are similar to applying dicing blades, as outlined in chapter 3.3.1. Advantages of applying macro grinding wheels are a higher process efficiency in terms of material removal rates, while the minimal producible structure dimensions are bigger than those applying dicing blades [61].

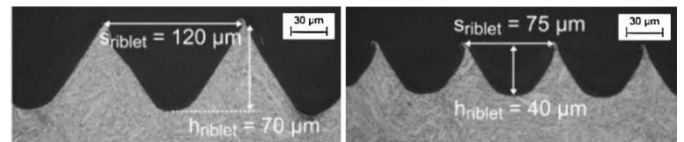


**Fig. 31.** Different possible riblet dimensions using profile grinding [61].

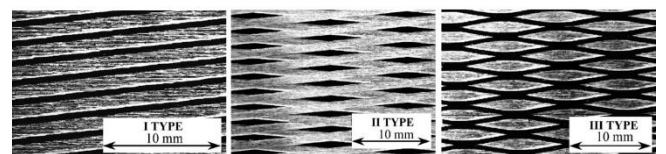


**Fig. 32.** Three types of the grooved surface (top view photographs) obtained with the wheels having helical grooves [217].

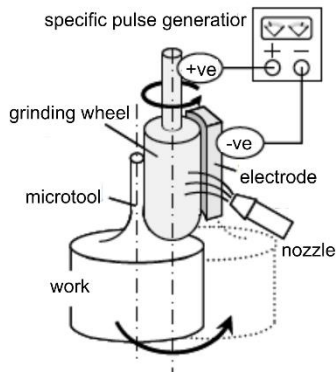


Fig. 33. Example of ELID grinding setup for generation micro-tools [177].

### 3.3.4. Electrolytic in-process dressing (ELID) grinding

As the precision and the capability of grinding micro-features is not only dependent on the machine tool precision but also on the resultant cutting forces, it is important to maintain the sharpness of the grinding wheel. One way to achieve this is by the use of electrolytic in-process dressing (ELID) grinding [118]. An ELID fabrication system was developed and its application by grinding micro-cylindrical and micro-angular shafts was studied [118]. Later, they optimized machining process conditions to improve surface characteristics of the prepared micro tools in nano-meter level, and a tum diameter tip was achieved [119]. The use of ELID grinding to generate micro-features/tool was reported (Fig. 33). The mechanical strength of fabricated micro tools should be adjusted by controlling surface characteristics [179]. Variety of shapes of ultra-fine micro-tools were fabricated, and the strength test results showed that the differences in surface characteristics had an extremely significant influence on its strength [178]. It was confirmed that ELID could be used to carry out micro-machining [134]. Cup-type wheels and ELID process were compared when doing precision grinding for spherical lenses and microspherical lenses and it was claimed that the ELID grinding could achieve better surface roughness and sharp accuracy [161]. From the published literature it has been observed that the process is capable in producing highly accurate features not only of revolution (Fig. 12 left) but also with sharp edges (Fig. 12 right) at high length-to-diameter ratios that are challenging to obtain by other mechanical material removal processes. These features can be machined at high precision in hard materials such as cemented carbides. Furthermore, this technology has been further proposed to be implemented on desktop-sized or miniaturised machines, facilitating the implementation of the process to wider micro-fabrication of high-value products, e.g. silicon wafers or moulds. The capability of the process has been proven further in fabricating polygonal tools (edge radii as small as  $1\mu\text{m}$ ) and surface roughness as low as  $1.8\text{nm Ra}$  (Fig. 12).

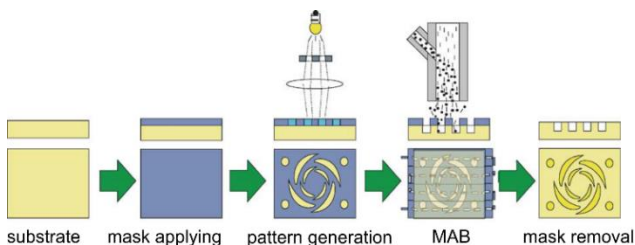


Fig. 34. Micro-Abrasive Dry Blasting [1].

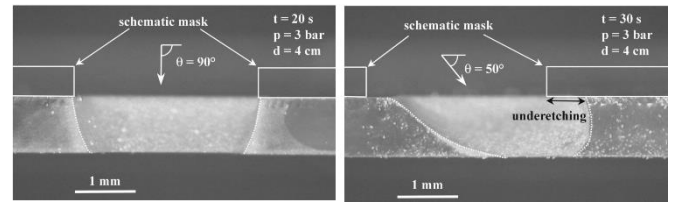


Fig. 35. Influence of nozzle obliquity in MADB [23].

## 3.4. Micro Abrasive Blasting

### 3.4.1. Micro Abrasive Dry Blasting

In *Micro abrasive dry blasting* (MADB), a mask is deposited above a substrate and blasted with a gas beam carrying high-velocity abrasive particles, as shown in Fig. 34. This method is well suited for machining of brittle materials such as glass and silicon, finding application in micro-electromechanical systems (MEMS). The transition from brittle to ductile removal on these materials is not sudden, occurring over at least one decade of kinetic energy [247]. Application to a number of other materials has been reported, such as acrylic and polycarbonate polymers for which ductile machining was observed [81]. Fundamental process parameters in MADB include the nozzle shape, its obliquity and distance from the workpiece, the type and size of abrasives, as well as the mask.

The influence of nozzle shape on erosion rate and profile was analysed by [67], in which it was found that round nozzles tend to machine profiles with a V-shaped cross-section, whereas rectangular nozzles display reduced flux effect, therefore resulting in more uniform removal profiles. Obliquity of the nozzle relative to the surface was shown to be an important factor [23]. Angles other than  $90^\circ$  result in varying levels of under-etching of the side-walls, as shown in Fig. 35, an effect which may or may not be desirable. Furthermore, for obliquity angles around  $55^\circ$  variations of the material removal has been observed as a factor of jet scanning direction [82].

Abrasive particles tend to follow a Weibull or piece-wise Weibull distribution across the nozzle outlet, with the jet being more focused as particle density increases [31]. The influence of particle size, velocity and attack angle was studied by [97], through single impact experiments. Based on experimental observations of lateral crack initiation, a relatively simple model was proposed that can predict the surface roughness  $R_a$  and erosion rate  $E_r$ :

$$R_a = \frac{a(3c_l^2 + 2a^2)}{12c_l^2} \quad (3)$$

$$E_r = \frac{\pi \rho_t a (a^2 + 3c_l^2)}{6 m_p} \quad (4)$$

$$a = \left( \frac{3U}{2\pi H} \right)^{1/3} \quad (5)$$

where  $m_p$  is the mass of incoming particles,  $a$  the size of indented zone,  $U$  the particle kinetic energy,  $H$  the substrate hardness and  $\rho_t$  its density, and  $c_l$  the lateral crack length. Reducing the kinetic energy of abrasive particles leads to lower surface roughness, a process variant that was exploited with shallow attack angles in finishing of brittle glass, and for which roughness improvement up-to 70% was reported [98,108].

Laser shadowgraph observations found a particle velocity through the mask that is constant, but significantly lower than in the free jet [58]. The influence of mask material was studied by [1], in which metals, elastomers and photo-resist were compared in terms of erosion resistance and shape transfer accuracy. Metals are recommended for high energy processing, elastomers allow for greater pattern complexity, while photo-resists offer a good compromise between these two extrema. The use of dual-layer has been explored [138], whereby a soft resin layer of high adhesion is

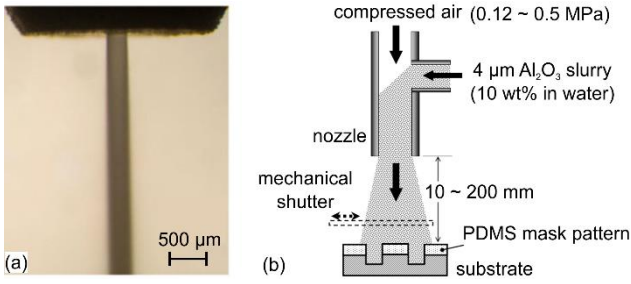


**Fig. 36.** (a) Micro abrasive slurry jet [94], (b) Air driven slurry blasting system [165].

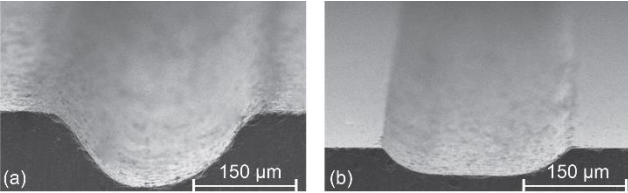


**Fig. 37.** Micro-channels machined with pump driven system (a) Without pulsation damper, (b) With pulsation damper [174].

deposited underneath a hard oligomer layer with high erosion resistance. To attain ultra-fine feature resolution, techniques such as laser-patterning [258] and lithography [201,248] have been employed for mask generation, with final abraded feature resolution in the range of 50 – 100 μm.

A selection of technical demonstrations are shown in section 2. MADB compares favorably with methods such as micro-end milling [274], ultrasonic fabrication [15], and wet-etching [189]. This is particularly the case in micro-structuring of brittle materials such as PZT micro-pillars [15] and glass micro-channels [205,259], with the latter showing electro-osmotic mobility remarkably similar to wet-etched channels [84]. Under-etching of the surface by oblique machining can produce complex monolithic structures such as glass cantilever beams [21,188]. Furthermore, micro-blasting of multiple substrates has been used in fabrication of intricate mechanical assemblies such a micro-pumps [264], and embossing molds for MEMS replication [144].

Several process enhancements have been proposed to increase the repeatability and uniformity of material removal in MADB. Aiming at stability of the abrasive particle mass flux, [85] proposed and demonstrated a mixing device within the pressure reservoir, that ensures powder remains loose and able to flow freely though the orifice to the air stream, while [107] showed that mass flow rate monitoring is possible by attaching an acoustic emission sensor to the target. [275] proposed intermittent injection of abrasives into the gas stream, to prevent accumulation of particles on the target area. [87] showed that high-frequency vibration of the target substrate leads to more uniform roughness and removal. As a more flexible alternative to deposited masks, a sliding crossed shadow mask was shown to generate sub-millimeter features [172]. Finally, MADB of elastomers and polymers, such as polydimethylsiloxane (PDMS) or polytetrafluoroethylene (PTFE) was found to be very slow or impossible at room temperature. This has led to the adoption of cryogenic techniques to enhance removal [83,91], by injecting liquid nitrogen into the abrasive jet to enhance brittleness of the substrate.

### 3.4.2. Micro Abrasive Slurry Jet

*Micro abrasive slurry jet* (MASJ) refers to several schemes in which a jet of abrasive particles and water impinges onto a substrate surface. Whereas in abrasive water jet machining

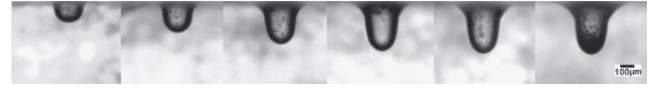


**Fig. 38.** Evolution of micro-hole depth with time [174].

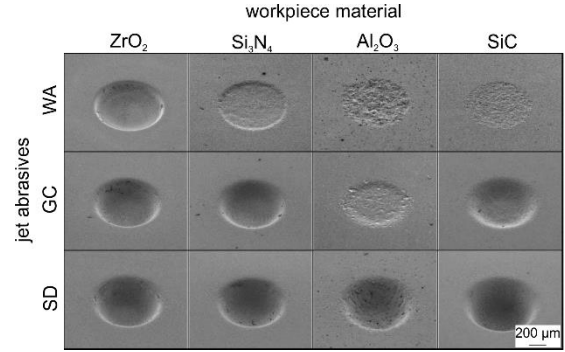


**Fig. 39.** Micro-holes machined for various abrasives/materials [235].

(AWJM) systems, a high-pressure pump (up-to 250 MPa) sends water into a mixing tube inside which abrasives are fed, in MASJ the abrasives and water are pre-mixed before being sent directly through a nozzle outlet. This pre-mixing allows for miniaturization of the nozzle to diameters as small as 250 μm [94], as shown in Fig. 36a, while preventing pre-mature erosion of the system components. An added benefit of pre-mixing slurry is the reduced amount of entrained air, as compared to AWJM, which results in a narrower slurry jet for comparable particle velocities. For micro-channels of a given depth, the width of those made by MASJ are typically 25% narrower than those produced by AWJM [93]. In some systems, compressed air may be used to draw slurry into the nozzle, and a mask applied to the surface in order to control the blasting area, as shown in Fig. 36b [165]. Fundamental process parameters in MASJ include the slurry pressurization system, nozzle obliquity and distance from the workpiece, the type and size of abrasives, as well as the mask. Assuming insignificant friction and contraction losses, the average slurry jet velocity  $v_s$  at the orifice exit can be estimated from Bernoulli's equation [175]:

$$v_s \approx \sqrt{\frac{2(P_h - P_a)}{\rho_s}} \quad (6)$$

where  $P_h$  is the hydrostatic pressure at the orifice entrance,  $P_a$  the atmospheric pressure, and  $\rho_s$  the slurry density. The MASJ process is particularly sensitive to fluctuations in slurry pressure. Fig. 37 shows SEM micrographs of micro-channels machined by a diaphragm pump driven system, with or without the addition of a slurry pulsation damper. Equalisation of the pressure leads to significantly narrower and uniform removal profiles [174]. Direct pressurisation of the slurry tank offers greatest stability, but has downsides such as limited volume of usable slurry [175].

Extensive studies on glass and PMMA were conducted by [173], in which the width and depth of micro-channels were found to increase as function of obliquity angle, orifice size, as well as abrasive particle diameter and density. However, increased slurry temperature led to narrower and deeper channels. Evolution of the micro-hole profile  $E(x)$  is generally governed by a partial differential equation given in [86]:

$$z_{,t^*}^* - E^*(x^*) \left[ 1 + z_{,x^*}^{*2} \right]^{-\left(\frac{k}{2}\right)} = 0 \quad (7)$$

where  $z^*=z/L$ ,  $x^*=x/L$  and  $t^*=t/T$  are the non-dimensional channel depth and width relative to a characteristic length  $L$ , the time constant  $T$  is a measure of the erosion rate at the centre of a shallow channel, and the velocity component  $k$  expresses dependence of the erosion rate on particle velocity [175].

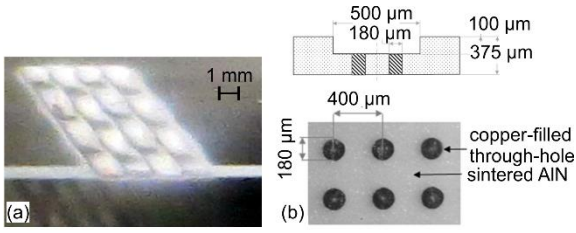


**Fig. 40.** Technical demonstrations of MADB (a) Undulating micro-channels [216] (b) AlN wafer with Cu filled holes [128].

This equation correctly describes the usual tapering of removal depth observed in experimental trials, as shown in Fig. 38. Return flow was identified as an issue, with secondary impacts of abrasives causing frosting damage to walls and non-targeted areas around the jet [173]. The solution is typically to mask non-targeted area with an epoxy coating.

The influence of abrasive and target material type was studied by [235], in which it was shown that conventional erosion models based on ideal crack formation fail to take into account the relative hardness of abrasives that is critical in MASJ. Fig. 39 demonstrates variations in micro-hole generation with alumina (WA), silicon carbide (GC), and synthetic diamond (SC) abrasives. It was further clarified that radial cracks do not tend to be generated under particle impact, thus preventing degradation of flexural strength in the machined target.

A numerical model for etching of three-dimensional features with prescribed topographies was described by [215], in which the inverse problem is expressed as a Fredholm integral equation of the first kind. The difference kernel is represented by the erosive function, while jet location and velocity are resolved.

A selection of technical demonstrations is shown in Fig. 40. Using the inverse problem method, undulating micro-channels (a) were imprinted without requiring a mask [216]. With a 2 steps process chain of MADB and MASJ, [128] was able to produce microchannels in AlN wafers with Cu filled through-holes (b). With the addition of a rapid abrasive suspension valve, [164] was able to produce microchannels in AlN wafers with Cu filled through-holes (b). With the addition of a rapid abrasive suspension valve, [265] was able to demonstrate drilling of 85 μm diameter holes in 50 μm thick steel at a rate of 2.5 holes per second and cutting 100 μm thin features without a mask.

A number of process enhancements have been proposed to improve material removal characteristics in MASJ. Firstly, the addition of long-chain polymers to the slurry results in non-Newtonian fluids with altered viscosity and elasticity. Addition of 50 wppm polyethylene oxide (PEO), the highest possible concentration before jet oscillation occurs, was shown to result in 21% narrower micro-channels [127]. Improved edge sharpness was also observed, and drilling of 3 mm thick glass sheet without chipping around the exit edge shown to be feasible [125]. Secondly, replacing water with an electrolyte of NaCl and NaNO<sub>3</sub> permits abrasive enhanced electrochemical jet machining. The synergy between mechanical and chemical effect leads to significantly higher material removal rate than either effect taken separately, and surface roughness somewhere between that achieved by the two separate processes [142]. This makes the process attractive for difficult-to-cut materials such as tungsten carbide [143].

### 3.4.3. Micro Abrasive Jet Polishing

*Micro abrasive jet polishing (MAJP)* refers to a process in which a pressurized mixture of fluid and abrasives is passed through a sub-millimetre sized nozzle at a relatively low pressure when compared to MASJ. The jet impinges onto the workpiece surface, which causes ductile removal of material by gentle impacting of the abrasive particles. Some advantages of MAJP include the ability to

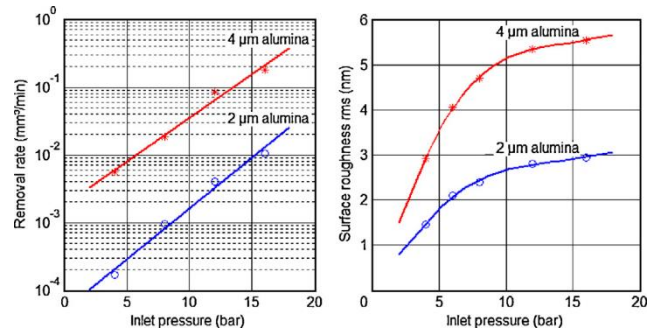


**Fig. 41.** Relationship between grit size and inlet pressure vs. removal rate and surface roughness in MAJP [17].

generate nanometer deep polishing footprints, reach difficult areas behind narrow gaps, such as boreholes and steeply concave optics, as well as a total absence of tool wear. Fundamental process parameters in MAJP include the slurry pressurization system, nozzle obliquity and distance from the workpiece, and the type and size of abrasives. The relationship between pressure and jet velocity is again well described by the Bernoulli equation.

Typical operating conditions range between 0.2 to 2.0 MPa, with corresponding fluid velocities in the order of 10-50 m/s. The relationship between inlet pressure, removal rate, and surface roughness has been described in the literature [17]: removal rate increases exponentially with inlet pressure, while surface roughness follows a more linear relationship, as shown in Fig. 41. MAJP is thus well suited for nanometer level surface finishing on a variety of materials, such as glass optics and electroless nickel plated dies used for injection molding of plastic lenses.

A comprehensive mathematical model of material removal in MAJP is available in [38]. The volume of material  $V$  removed by a single particle can be expressed as a simple function of its mass  $m_p$  and impact velocity  $(v_x, v_y)$ :

$$V(v_x, v_y) = k \left( \frac{1}{2} m_p v_x^2 \right) \left( \frac{1}{2} m_p v_y^2 \right)^{\frac{2(1-b)}{3}} \quad (8)$$

where  $k$  is a workpiece material coefficient accounting for plastic flow pressure and spring back, and  $b$  ( $0.5 < b < 1$ ) is a material dependent exponent of the cutting cross-section area. Distribution of removal across the jet footprint  $E(r)$  is then expressed as:

$$E(r) = \sigma_a(r) V(v_x(r), v_y(r)) \quad (9)$$

where  $\sigma_a(r)$  is the particle density, which together with particle velocities can be derived from computational fluid dynamics modelling [18]. The predictability and stability of material removal in MAJP have led to its adoption in nano-shaping of functional surfaces, through moderation of jet feed by a dwell-time algorithm [70]. A potential issue in MAJP is the tendency for abrasive particles to penetrate the substrate materials and remain embedded on the surface. This is especially the case when processing softer materials such as nickel alloys. In the case of harder materials, such as ceramics, grain dislocation may occur if the processing conditions are too harsh on the substrate. Both issues have been documented, and can be predicted and avoided through the application of simple criteria [19].

A selection of technical demonstrations is shown below. MAJP has a propensity for removing fine tool marks, which makes it a useful process in applications where cutting, turning or blasting marks may cause degradation of the optical performance (due to light diffraction). Examples include small aspheric diamond turned electroless nickel moulding dies [17] and micro-grooves few hundred nanometre wide and few dozen nanometre deep such as shown in Fig. 42 [160]. By application of the dwell-time method, polishing of functional micro-structures with sub-millimetre

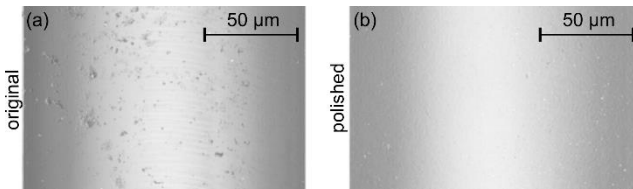


Fig. 42. MAJP polishing of micro-grooves [160].

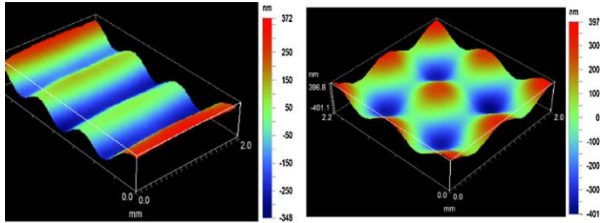


Fig. 43. MAJP polishing of functional micro-structures [39].

feature resolution was demonstrated by [39], as shown in Fig. 43. A number of enhancements to the basic MAJP process have been proposed and demonstrated. [227] describes the use of magnetorheological fluid that stiffens under the influence of a magnetic field. In this method, the well collimated jet can achieve a higher degree of accuracy in targeting the polishing zone. Corrective polishing down to few tens of nanometre peak-to-valley in form accuracy was demonstrated by this process. [243] describes a specially shaped MAJP nozzle with micro-holes, that is pressed very close to the workpiece. As the fluid flows out of the micro-holes, the small gap forces it to flow tangentially to the workpiece surface, thus yielding very low surface roughness in the order of few Angstroms rms.

To enhance the removal rate, mixing of air with the abrasive slurry was proposed. The setup implemented by [163] consists of a simple pulsating air supply and mixing valve, while [105] draws slurry into an air stream by Venturi effect. In both cases, the removal rate increases by at least one order of magnitude, but surface roughness worsens by two orders of magnitude. In order to solve this surface roughness issue, [16] proposed generating micro-bubbles inside the nozzle cavity by ultrasonic cavitation. In this setup, removal rate increases by up-to 380%, while surface roughness remains unchanged as compared to standard MAJP.

Finally, a more basic idea for enhancing removal rate consists of building an array of micro-jets, such as demonstrated by [240]. In this configuration, it is possible to polish arrays of micro-lenses simultaneously, without any significant loss in process controllability or accuracy. In another implementation, a spinning head fitted with confocal jets arrayed around the rotation axis was demonstrated [209] to improve surface roughness on optical glass.

### 3.5. Vibration assisted Micro Machining

In 1997, ultrasonic vibration-assisted micro machining (micro UM) was significantly advanced by creating a micro-tool and adding tool rotation to create *micro rotary ultrasonic machining* (micro RUM). Rotating the micro-tool in micro RUM reduced the tool runout caused by inaccurate tool mounting, but the rotation required ultrasonically vibrating the workpiece instead of the micro-tool [114]. Further advancement enabled the machining of 5 μm diameter holes in quartz glass [65]. In addition to the improved machining accuracy, the enhanced debris removal resulting from the tool rotation led to an increased material removal rate [272].

The diameter of the tool in micro RUM is between 100 μm and 300 μm. The tool generally rotates at 1000-3000 min<sup>-1</sup>, and the workpiece vibrates at a frequency of 20-100 kHz with an

amplitude of 0.5-5 μm [218,272]. The vibrating workpiece causes the abrasive to impact the workpiece ultrasonically, which generates the surface (e.g., drills or slots). A tungsten, tungsten carbide, or stainless-steel tool is used, while loose abrasives (grain size: 0.5-5 μm) with the mixture of water or oil is used as abrasive slurry. Machining with fine abrasive slurry results in a fine surface finish, and use of an oil-based slurry results in a smoother surface finish than a water-based slurry [52]. Tool wear in micro RUM causes deterioration of the material removal rate and machining accuracy. The tool wear could be due to the direct contact of the tool against the workpiece, the impact and cutting of the abrasive particles, and the ultrasonic cavitation. However, theoretical and experimental analyses have revealed that low-cycle fatigue of the tool, caused by the repeated abrasive impacts, is the dominant cause of tool wear [273]. Moreover, experimental analysis demonstrated that the rotational speed of the tool does not significantly influence the tool wear [273] or the material removal rate [218].

Another application using loose abrasive is called micro ultrasonic vibration assisted lapping (MUVL) [238]. This method is designed to improve the dimensional accuracy—especially roundness of holes drilled using micro EDM. In MUVL, a micro-tool is inserted into a hole, rotated, and vibrated at a high frequency (e.g., 30 kHz.), driving the abrasive into the gap between the tool and the wall surface of the hole to remove the recast layer generated during micro EDM. It has been reported that a minimum roundness of 1 μm was achieved using MUVL in a micro hole poorly drilled using micro EDM in a titanium alloy (Ti-6Al-4V) with a 70 μm diameter tungsten carbide tool [238].

Because of the advancement of micro-tool technology, bonded abrasive (electroplated diamond tool) can be used in micro RUM, in addition to loose abrasive (abrasive slurry). While the loose-abrasive method is commonly used to machine relatively shallow features (~60 μm deep), the bonded abrasive method enables the machining of deeper features (more than 100 μm deep) [199].

In the bonded-abrasive case, an electroplated micro diamond tool (abrasive size: 5-120 μm) is commonly used. Either tool or workpiece can be ultrasonically vibrated. The rotational speed of the tool can be 5000 min<sup>-1</sup> or more [181,199]. However, unlike the abrasive-slurry case, the rotational speed of the tool influences both tool wear and material removal rate. Increasing the rotational speed of the tool increases the material removal rate and decreases the rate of tool wear [109,199].

The applications of micro RUM include not only drilling and grooving but also the fabrication of micro carbide tools (11 μm in diameter and 160 μm in length) [182] and a carbide rod with aspect ratio 310:1 and diameter 42 μm [257]. The fabrication of thin, tens of micrometer thick SiC diaphragms for pressure sensors using ultrasonic vibration mill grinding is a novel application [136]. Those initial applications have been also extended to include ductile materials such as stainless steel [181], and biomedical materials such as bovine ribs [198].

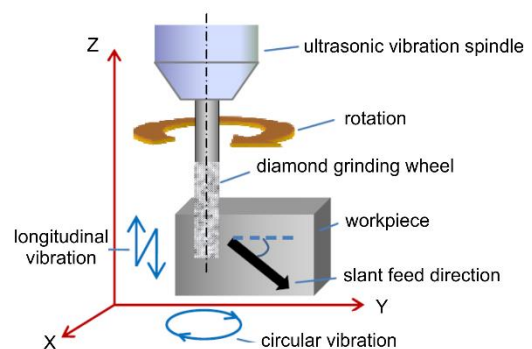
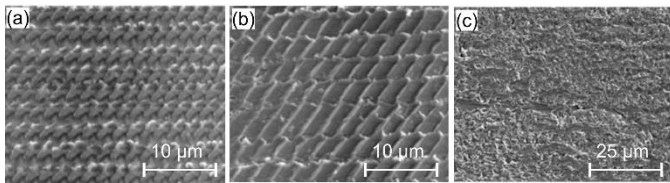


Fig. 44. Ultrasonic vibration assisted slant feed grinding [256].



**Fig. 45.** Typical textured surfaces fabricated by UASG respectively using (a) 1D, (b) 2D, and (c) 3D vibration modes [255].

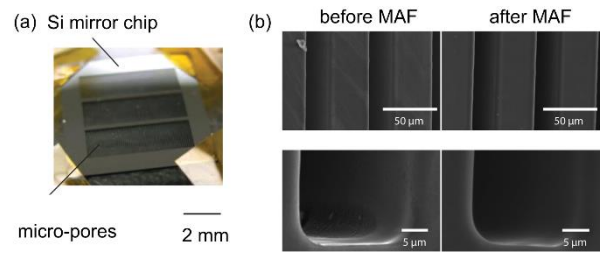
Recent advancements in micro RUM have resulted in new research areas, such as fabrication of micro/nanometer-scale structures (*ultrasonic-assisted texturing*) for surface functionalization on ceramic surfaces [255]. In ultrasonic vibration-assisted grinding, the grinding wheel is vibrated in only one dimension (1D) to fabricate micro-features (diameter: 11-23  $\mu\text{m}$ ; length: 50-320  $\mu\text{m}$ ; aspect ratio: 3-18) [182], but the grinding wheel is vibrated in two or three dimensions in ultrasonic-assisted texturing to create the resulting surface textures. Fig. 44 shows an example of ultrasonic-assisted texturing called *ultrasonic-vibration-assisted slant-feed grinding* [256]. In this method, three grinding-wheel vibration modes are available: reciprocation in the longitudinal direction (1D), circular or elliptical vibration (2D), and a combination of reciprocation and circular vibration (3D).

Fig. 45 shows surface textures fabricated on zirconia surfaces using 1D, 2D, and 3D vibration modes. While the textures made using 1D and 2D vibration modes are periodical, the texture made using 3D is random. These micro/nanometer-scale structures are a unique aspect of grinding technology, and they are different from the structures made using ultrasonic vibration-assisted cutting [255].

### 3.6. Magnetic Field-Abrasive Finishing

*Magnetic field-assisted finishing* (MAF) is used to process surfaces by moving abrasives mixed with a mass of ferromagnetic materials (e.g. ferrous particles) suspended in a magnetic field. The process parameters are the magnetic field, which determines the tool's relative motion against the target surface and the force acting on the tool (the dominant component of the finishing force). Depending on the application, either a static or an alternating magnetic field can be used. While a static magnetic field encourages tools to slide over the target surface, an alternating magnetic field encourages tools to collide against the target surface. The magnetic force acting on the tool is expressed as the product of the volume of the tool, its magnetic susceptibility, the magnetic field intensity, and its gradient. The force acting on the tool is easily altered by changing the size of the tools, and the application of the tools is determined based on the magnetic force required for processing. Magnetic fluid, a colloidal suspension containing magnetic nanoparticles, magnetorheological fluid, a fluid with carbonyl iron particles of several micrometers in diameter dispersed in it, and ferrous particles, between tens and hundreds of micrometers in diameter are representative tools. The use of magnetic fluid generally achieves nanometer-scale surface finish. E.g. a mixture of magnetic fluid and 0-1  $\mu\text{m}$  diamond abrasive was vibrated at an amplitude of 100  $\mu\text{m}$  and a frequency of 20 Hz over a borosilicate (BK-7) glass workpiece. After processing for 5 min, a  $\sim 2.3 \mu\text{m}$  deep,  $\sim 400 \mu\text{m}$  diameter depression was created and a roughness of 60 nm  $R_{\text{max}}$  was achieved [230].

When subjected to an alternating magnetic field, a mixture of magnetic fluid and abrasive slurry was alternately attracted by the magnetic pole; the pore sidewall surfaces were finished as the



**Fig. 46.** (a) Mirror chip and (b) sidewall surfaces of micro-pores before and after MAF [194].

mixture was forced into the micropores (10 or 20  $\mu\text{m}$  wide and 300  $\mu\text{m}$  deep), originally machined using LIGA or deep reactive iron etching (DRIE) [195,196]. As shown in Fig. 46, the sidewall surface ( $\sim 35 \text{ nm } R_q$ ) was smoothed to 1.7 nm  $R_q$  by hydrogen annealing and subsequently finished to 0.18 nm  $R_q$  by MAF using the mixture of magnetic fluid and 20 nm mean diameter colloidal silica [195].

The use of magnetorheological fluid enables nanometer- to submicrometer-scale surface finishes. An example is the surface finishing of complex microchannels in a copper substrate. The microchannels varied in width and depth in the ranges of 0.25-2 mm and 22.7-60.6  $\mu\text{m}$ , respectively. The bottom surface of the channels was smoothed from 0.86-1.52  $\mu\text{m } R_a$  to 0.25-0.78  $\mu\text{m } R_a$  [110].

Some applications, such as surface and edge finishing of difficult-to-machine materials (including stainless steels, high-speed steels, and cemented carbides) require much higher finishing forces than those commonly generated by magnetic and magnetorheological fluids. In those cases, ferromagnetic particles (ranging between tens and hundreds of micrometers in diameter), ferromagnetic particles mixed with abrasive grains, or composites of iron and abrasive (alumina or carbides, etc.) are applied in a static magnetic field to generate the forces necessary to facilitate machining. The force per processing area for micromachining applications are generally between 10 kPa and 40 kPa, and the resulting surface roughness is typically on the submicrometer order.

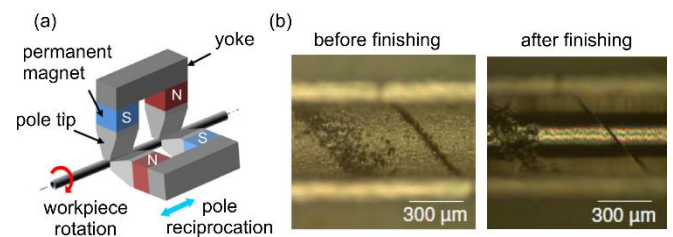


**Fig. 47.** (a) Schematic of magnetic abrasive finishing process using multiple pole-tip system (b) Internal surface images of flexible catheter shaft (0.58 mm OD, 0.42 mm ID) finished by MAF process [115,260].

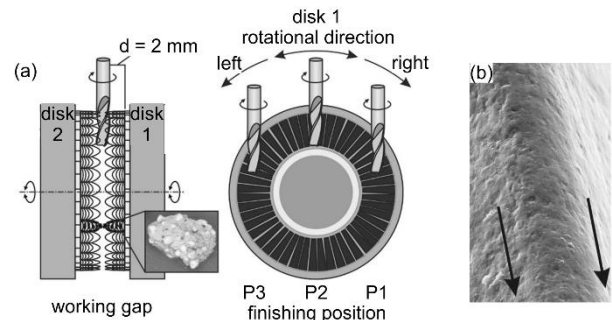


**Fig. 48.** (a) Schematic of processing principle and (b) a SEM micrograph of cutting edge of tool after finishing [60].



A representative example is the internal finishing of 304 stainless steel capillary tubes (400  $\mu\text{m}$  ID), which are widely used for medical devices and equipment. Finely finished surfaces are desired to facilitate smooth flow of fluid or tissue inside the tube. The as-received surface,  $R_a$  of 0.26  $\mu\text{m}$ , was smoothed to 0.02  $\mu\text{m}$  [261]. To improve the finishing efficiency of MAF, methods to simultaneously finishing both internal and external surfaces of capillary tubes [176] and finishing multiple areas using multiple pole-tip systems [115] have been proposed, as shown in Fig. 47a. The flexibility of catheter shafts is controlled by slots and patterns machined into slender stainless-steel tubes by lasers. Resulting burrs and adhered material must be removed to allow flexible motion of the shaft. The method shown in Fig. 47b is also applicable for the interior surface and edge finishing of flexible catheter shafts [260].

Edge preparation of cutting tools such as drill bits, cutting inserts, and milling cutters is another application. Fig. 48 shows a case using a static magnetic field [60]. Magnetic abrasive particles generate a particle brush between two coaxial disks equipped with permanent magnets. When the disks rotate, the magnetic abrasive brush moves relative to the cutting tool inserted into the brush. In contrast, an alternating magnetic field-assisted machining process has been used to make metastable 304 stainless steel tools collide with the tool cutting edges, removing some excess material. [53] reported that the cutting-edge radii of twist drills were slightly modified from 3-11  $\mu\text{m}$  to 18-50  $\mu\text{m}$ .

#### 4. Modelling of small-scale material removal processes

As outlined in section 3.2, the fundamental principles involved in the small-scale material removal process could be further assessed by modelling techniques. This chapter gives an overview of the current state of the art of modelling approaches.

According to [100], an abrasive process can be classified as path bound, force bound or energy bound. Accordingly, in this section, to explain the different modelling approaches for various abrasive processes, they are classified mainly as two types:

- (i) bonded or fixed abrasive processes (path bound)
- (ii) unbonded or loose abrasive processes with an actuation mechanism (force bound or energy bound)

##### 4.1. Modelling of bonded or fixed abrasive processes

Processes such as grinding, honing, brushing, abrasive sawing, and belt finishing etc., belong to the bonded abrasive process type, and modelling of these processes were explained in earlier keynotes [30,214] and other review articles [60,237]. Here, only abrasive processes which are used for micro parts and microstructures as classified in section 3 are considered.

In spite of the considerable number of experimental works published, theoretical and modelling works are very limited in micro-grinding. According to [90], lack of physical information establishing the relationship between the physical and mechanical properties of the machined materials, the deformation rate, and the non-steady temperature field in the contact zone, all limit the modelling accuracy.

According to [187], in micro-grinding process the values of contact length and temperature in the contact zone vary proportionately with the size of the wheel. However, ploughing phenomenon inversely varies with the size of the wheel. Hence, effects related to ploughing component needs to be taken care of specifically. In line with this variation, a semi-analytical model (combination of analytical model and empirical model) for predicting micro-grinding forces that considers the mechanical and thermal effects interaction and size effect at the microscale

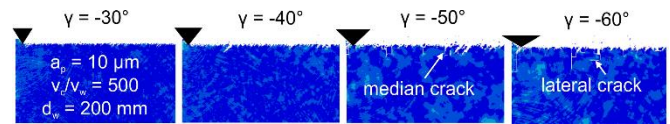


Fig. 49. Effect of different rake angles on SSD [191].

level of material was developed [187]. With this methodology, the micro grinding forces based on micro-grinding wheel topography and material properties was quantitatively predicted.

Finite Element (FE) and molecular dynamic (MD) simulations based on single grain scratch test have been extensively developed to understand microscopic material removal mechanism. A 2D FE model for studying subsurface damages in BK7 glass, is shown in Fig. 49 [191]. With this model interdependencies of the process kinematics, the tool's and grain's geometric properties and the crack propagation and sub-surface damage were identified. Another 3D FE model was developed to study the material removal mechanism in brittle materials (BK7 glass) [239].

The influence of micro pencil grinding tool topography on micro channel geometrical deviations was studied using kinematic simulations [206]. Results emphasized the influence of maximum protruded grits radial positions and the number of grits on geometrical deviations of the produced channels.

To further understand material removal mechanism with the interaction of liquids and gasses, nanoscale and atomic scale molecular dynamic simulation were developed. Similar to the majority of FE simulations, molecular dynamics simulations consider single grit scratching. Hence, results obtained from these simulations could be applied to the mechanism of both bonded and unbonded abrasive processes. The majority of MD simulation works are confined to understanding the ductile-brittle transition behaviour of brittle materials. A detailed review of MD simulations relevant to machining processes is compiled in [88]. To study the ductile-brittle transition of monocrystalline silicon at the nanoscale, a molecular dynamic study with different edge radius and undeformed chip thickness combinations was applied [35,36]. The results showed that as the undeformed chip thickness is larger than the cutting edge radius, in the chip formation zone there is a peak deformation zone in association with the connecting point of the tool rake face and tool edge arc. The interatomic bond length's increase in the peak deformation zone results in volumetric expansion of the zone. This can cause the neighbouring material to be tensily stressed, leading to crack initiation in the material in which the tensile stress is nearly perpendicular to the direction from the connecting point of tool edge arc and tool rake face to the peak. If the undeformed chip thickness is smaller than the cutting edge radius, there is no peak in the chip formation zone, and thus there is no crack initiation zone in the undeformed workpiece material. These findings explain well the phenomena of ductile-brittle transition associated with undeformed chip thickness and edge radius, as explained in section 3.2.

Similarly, in [252] a nanoscale molecular dynamic study to understand the ductile-brittle transition behaviour in SiC material with diamond grits and different undeformed chip thickness values was conducted.

MD simulations at atomic level (depth of cuts: 4 Å, 8 Å, and 12 Å) were applied to understand the chip formation, grinding forces, and temperature of the copper material. The simulation results indicate that with the increase of the depth of cut, average cutting forces increase and therefore temperatures at the contact zone are similar to conventional grinding findings [154].

##### 4.2. Modelling of unbonded or loose abrasive processes

A framework and unified modelling approach for various unbonded abrasive processes was discussed in an earlier keynote

paper [100]. Therefore, here only modelling and simulations efforts related to micro-abrasive blasting, vibration and magnetic field assisted micro-machining process are discussed.

In magnetic field assisted abrasive process, there are several parameters which can affect the result at the macroscopic and microscopic level [100], also mentioned in section 3.5.

Magnetic field assisted processes is a force bound process, in which the strength of the magnetic field decides the grain penetration depth and in turn all other process responses. Hence, in the modelling of magnetic field assisted finishing processes, many researchers have attempted to first understand the strength of the magnetic field by FE simulations, as well as physical, mathematical or empirical modelling, and then proceed towards force modelling and ultimately the material removal and workpiece properties.

The smoothed particle hydrodynamics (SPH), a mesh-free numerical technique, was used to simulate ultrasonic machining of float glass material [241]. Additionally, propagation of cracks in substrates and fracturing of abrasive particles were also covered. In SPH method, the system is represented by a set of particles, which are carrying material properties and interacting with each other according to the governing conservation equations. It has some potential advantages compared to the conventional grid-based Lagrange techniques such as FEM, including the suitability for solving problems involved in large deformations and fractures, as errors due to mesh distortion and tangling can be avoided. Results suggested that harder and spherical shaped abrasives increase the material removal efficiency. Furthermore, spherical shaped  $Al_2O_3$  grit result into improved surface integrity, as shown in Fig. 50.

A numerical investigation using the dynamic meshing technique in Computational Fluid Dynamics (CFD) was carried out for ultrasonic-vibration assisted micro-channelling process on glasses by an abrasive slurry jet [190]. The effect of ultrasonic vibration on the stagnation zone, the particle impact velocity and impact angle, and viscous flow induced erosion process was investigated. It was observed that the static pressure in the stagnation zone, particle impact velocity and impact angle are varied periodically with the assistance of the ultrasonic vibration on the workpiece which in turn could affect the material removal process. It was also found from the simulation that the ultrasonic vibration is beneficial to the viscous flow induced erosion during the low-pressure abrasive slurry jet micro-machining process.

In another work, CFD simulations were performed to study the erosion behaviour of glass surfaces in the vibration-assisted abrasive slurry jet machining process. The Eulerian-Lagrangian method and dynamic meshing technique are used to represent the abrasive slurry jet flow and the periodical movement of the

workpiece, while the particle rebound model and semi-empirical erosion model for glasses by considering the brittle-ductile transition are employed to simulate the impact of the erosion process, respectively. From simulations, it was observed that the combined effects of stagnation zone and brittle-ductile transition results in W-shaped cross-sectional profiles. Application of ultrasonic vibration to the workpiece enlarges the machining area as well as erosion rate. Similar to those works CFD simulations were used to predict the erosive footprint size in abrasive jet micro-machining [126]. The footprint was found to be a result of both primary particle impacts in the conical plume emanating from the nozzle and secondary particle impacts driven by the flow. The footprint depended on target curvature because the spread in lateral particle rebounds differed, depending on the target radius. It thus follows that footprints obtained from shallow channels machined on flat targets cannot be used to predict channel shape on curved surfaces. In energy bound abrasive jet assisted process, most of the modelling and simulation works are confined to predicting the jet footprint area, erosion rate and channel geometry.

In [113] the FE method was used to calculate the distribution of magnetic field between the magnetic poles in which a cylindrically shaped workpiece was placed in electro-chemical magnetic-abrasive machining process. The cutting forces responsible for abrasion were calculated from the magnetic forces developed from the gradient of the magnetic field in the working gap. The effect of electrochemical and abrasion-assisted dissolution were incorporated into a roughness model using average anodic current empirical relation and revealad relations between electromagnet current, surface roughness and material removal.

In [42] a low-pressure abrasive flow polishing (LAFP) technology was presented to address the issue of finishing rectangular microgroove of Cu and SUS304 materials. The effects of abrasive flow on the polishing efficiency and uniformity were analyzed numerically using ANSYS Fluent. The rectangular structure of the polished microchannel was optimized by simulating the trajectory and erosion action of particles. The distributions of turbulence intensity and shear force in the polishing microchannel were analyzed and optimized.

The effect of alumina particles kinetic energy and jet impact angle on the roughness and erosion rate of channels machined in borosilicate glass using abrasive slurry jet was investigated in [96]. A CFD model was used to calculate the local particle impact velocities and angles, and thus the kinetic energies of particles striking the surface. The measured erosion rate at various impact angles and the observed damage due to individual alumina particle impacts indicated that the dominant mode of material removal was brittle erosion. Based on the CFD results, analytical brittle-erosion models have been developed for air assisted abrasive jet micromachining.

A surface evolution model was developed to predict the profiles of micro-channels and holes machined in borosilicate glass [174]. The results showed that, despite the differences in abrasive flow patterns between air and slurry-based systems, the surface evolution model developed for air-based systems accurately predicted the profiles of micro-channels produced in the slurry-based system with a maximum error of 7% for aspect ratios (depth/width) of up to 5. The predicted profiles of holes were also in reasonable agreement with a maximum error of 14% for aspect ratios close to 1.

FE simulations combined with the Monte Carlo method were conducted to predict the average shape of abrasive waterjet footprints and the variability along the trench [146]. For that purpose, the relevance of each random parameter, such as shape (sharpness), size and relative orientation of the abrasive particles, were investigated through parametric studies on these variables.

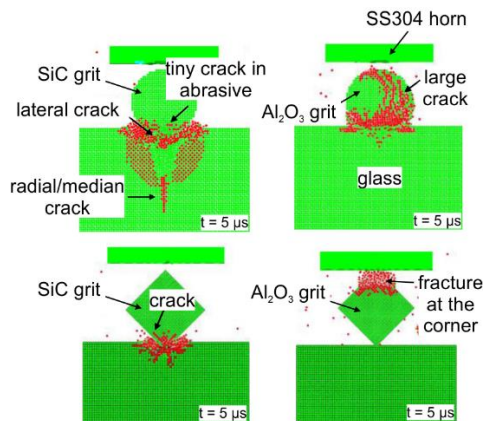
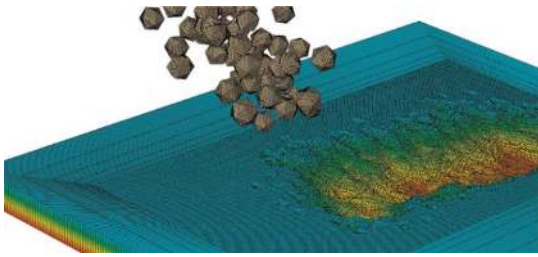
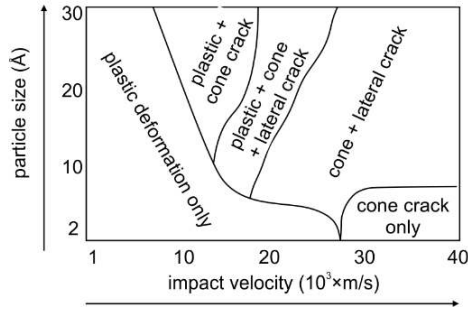


Fig. 50. Result of AUTODYN simulations for USM after 5  $\mu s$  with different abrasive grits and shapes [241].



**Fig. 51.** Snapshot of a simulation of one single trench using icosahedral particles at a velocity of 2000 mm/min with a tilted angle of 40° [146].



**Fig. 52.** Different regimes of material removal in VANILA process [111].

This process was simulated using Abaqus 6.14, in which multiple garnet particles hit the Ti-6Al-4V surface with very high velocity and erodes the target by plastic deformation and material removal as shown in Fig. 51.

Molecular dynamic simulations were conducted to study the Vibration Assisted Nano Impact-machining by Loose Abrasives process, which combines the principles of vibration-assisted abrasive machining, and tip-based nano-machining [111]. MD simulations were performed in this study to understand the effect of critical process parameters such as impact velocity, particle size, and the angle of impact of the abrasive grain on the material removal. A material removal mechanism map, capturing the effects of impact velocity and abrasive grain size on the occurrence and transitions between plasticity-dominated and fracture-dominated behaviours was derived (Fig. 52).

The abrasion phenomenon at atomistic and nano level under different contact pressures considering two-body and three-body contact sliding as shown in Fig. 53 was studied by means of molecular dynamics simulations [64]. A comparison between the simulations in Fig. 53(a), which was obtained with three-body contact sliding at low load, and the one in Fig. 53(i), which is the result of two-body contact sliding with cubic abrasives at high load, clearly shows the formation of wear particles in the latter case. The distinct horizontal grooves in Fig. 53(b) and Fig. 53(c) occur due to interlocking of neighbouring abrasives, leading to effective two-body contact sliding of one of the particles as its rolling motion is constrained. The grooves are perfectly horizontal because in the three-body contact sliding simulations, the only kinematic constraint on the abrasives is the motion in x direction while the motion in y direction results mainly from the current local topography. This work allows to evaluate the wear volume and the real contact zone resulting from two-body and three-body wear of nanoscopically rough surfaces during abrasion.

Molecular dynamics (MD) simulations were extensively done for polishing operations to analyze the material removal mechanisms. The impact of large porous silica cluster on silicon substrate, with different pore diameters was analysed as shown in Fig. 54 [44].

It was reported that, with the increasing pore diameter of the porous cluster, the number of the atoms removed from the impact silicon surface would firstly increase and then decrease until the

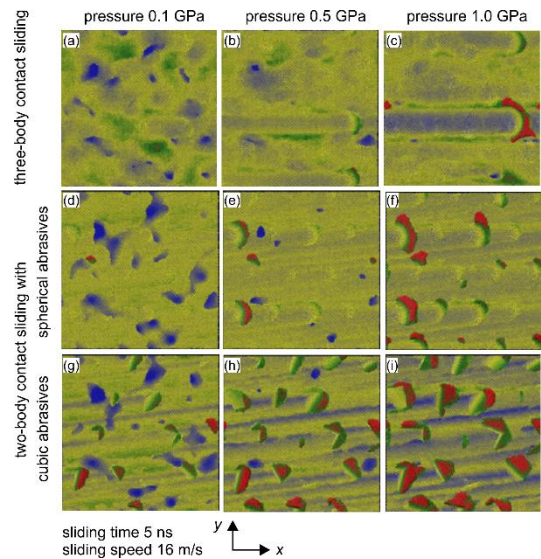


**Fig. 53.** Top view of surface topographies at various sliding conditions [64].

cluster adheres to the substrate. In addition, it was found that the effect of an enlarged real contact area between the cluster and the substrate is more significant than that of deeper penetration of the cluster in order to enhance the material removal rate during the impact. These findings were useful in optimizing the process parameters to obtain lower surface roughness and higher material removal rate during the chemical mechanical polishing process.

MD simulations at the atomistic level were used to study the interaction between silicon wafers with a diamond abrasive in a polishing process under dry conditions [3]. Simulations were conducted with silicon asperities of different geometries, different abrasive configurations, and polishing speeds. Under the conditions of polishing, silicon atoms from the asperities were found to bond chemically to the surface of the diamond abrasive. Continued transverse motion of the diamond abrasive (relative to the silicon asperity) leads to tensile pulling, necking, and ultimate separation of the silicon asperity material instead of conventional material removal in polishing (chip formation) involving cutting/ploughing, which takes place in the absence of chemical bonding between the abrasive and the asperity material.

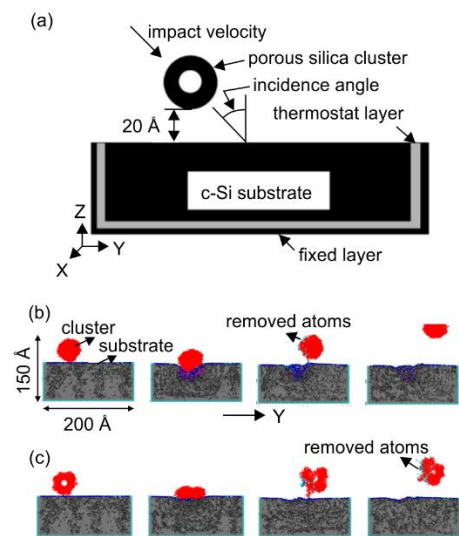


**Fig. 54.** (a) schematic diagram of a porous silica cluster impacting on the crystal silicon substrate for a molecular dynamics simulation (b) side cross-section view of the impact zone at the different moments at 4313 m/s and 45° of (b) P0-Cluster (c) P15-Cluster [44].

Rolling of an abrasive grit across a silicon surface with an asperity under various down forces and external driving forces were studied using molecular dynamics (MD) simulation [211]. It was shown that both the downforce and the driving force influence the amount of material removed. The changes in potential energies and kinetic energies of the particle and the silicon substrate during the abrasive rolling process attributed to the deformations and the rise in temperature of the particle and the substrate. According to the MD simulations, substantial hydrostatic pressure induced at the local area of silicon wafer forces the silicon atoms to transform from the classical diamond structure ( $\alpha$  silicon) to metal structure ( $\beta$  silicon) [99]. This important factor results in the ductile fracture of silicon and ultimately in a super-smooth surface.

The impingement of abrasive particles in water jet on a monocrystalline silicon substrate was studied by MD simulations [43]. The results show that as the standoff distance increases, the jet will gradually diverge. As a result, stress region and high-pressure region of the silicon substrate under small standoff distances were significantly larger than those under large standoff distances. Therefore, the material removal rate at the beginning will be high and then decreases due to an increase in the standoff distance.

## 5. Current status and future scope

In this chapter, the available manufacturing methods are reflected concerning their current possibilities to machine the products and applications introduced in chapter 2. Future research and development needs necessary to further exploit the possibilities of micro abrasive processes are identified.

### *Chip formation and ductile/brittle transition*

Models and knowledge on chip formation in micro abrasive processes is commonly derived from or equated with findings of macro grinding. In fact, the models and theories on cutting mechanisms in macro grinding are also not based on the observation of the process itself, in contrast to those of cutting processes like turning or milling, as the contact zone in grinding cannot be observed. They are based on chip root examinations, interrupted cutting or grain breakouts, single grain scratch tests and analogies to the theories of cutting with defined cutting edges. Such investigations are hardly possible on the small scales of micro abrasive processes. Also, to be able to give statements on e.g. uncut chip thickness values, equations are used that necessitate tool characterizations, which are also an issue on small scales. This could be an explanation on the deviation of the absolute values of the critical chip thickness to achieve ductile mode grinding comparing macro and micro grinding of the same material. Further research has to address these basics of chip formation on the micro scale and should include detailed quantitative characterization methods of tools and processes. To avoid the intricacies of the small scale of experimental conditions, the possibilities and current developments on modelling of the process, as outlined in section 4, could be exploited.

### *Abrasives*

While the advances in abrasive materials (e.g. crystallographically oriented structures) and their property customisation need to be transferred to the micro-tool design, it could be commented that the existing solutions might obtain abrasive grits or elements at the micro-scale level. It is believed that manufacturing technologies like laser ablation could generate, at competitive outputs and costs, such micro-abrasive elements (at order of microns rather than tens/hundreds of microns) of orderly distributions and controlled shapes. This will enable micro-grinding technology to make a leap forward in achieving tighter part quality measures. Nevertheless, it is felt that the technologies

of generating micro-abrasives by post-processes might induce additional form deviations of the tool geometry with negative influence to the precision of these micro-grinding tools. Hence, additional measures for getting the tools into the necessary tolerances (e.g. runouts) might be necessary in these conditions which will add to the overall cost of the technology.

### *Dicing Blades and Wire cutting*

For fine slotting using dicing blades and wire cutting it seems that significant research is needed to better understand how the quality of the edges and walls of the cuts can be improved. Here, some directions of research could be the customisation of the abrasive materials distribution on the edges and fronts of the dicing blades to address the differences in the cutting mechanisms occurring on the different areas of abrasive tools. Furthermore, geometrical customisation of the active surface of these abrasive tools could be realised to enhance the swarf removal and thus, cleaner cutting.

### *Micro Pencil Grinding Tools (MPGT)*

MPGT are a promising technique for micro structuring of hard and brittle materials at high flexibility concerning shapes and sizes. The challenge here is currently the targeted and repeatable coating of the tools. Further, detailed studies on the coating parameters and the coating composition are necessary to fully exploit the tool's potential. Tool optimizations also have to address the tool base body. On the one hand, shaping the base body can help to decrease clogging issues and to improve the bottom surface quality of the manufactured structures. On the other hand, tool breakage could be reduced by introducing new base substrates of the tools. Finally, wear of tools can be reduced by proper cooling. Research efforts should be directed in developing cooling strategies adapted to the process. This includes the coolant supply system but also the composition of the coolant itself.

### *Vibration assisted Micro Machining*

Recent study of *micro rotary ultrasonic machining* (micro RUM) has explored process applications from drilling and grooving of hard, brittle materials to surface texturing including fabrication of complex features used for MEMS, microfluidics, and sensor applications. However, methods and mechanisms to improve the quality of surfaces and subsurface created using micro RUM have not been reported. These areas should be part of future research, in addition to studying micro-feature fabrication characteristics and tool wear.

### *Micro Abrasive Blasting (MAB)*

Current laser drilling technology can produce nozzle insert for MAB with outlet diameter around 50  $\mu\text{m}$ , which allows for lateral processing resolution of around 100  $\mu\text{m}$ . Scope for further miniaturization of nozzles, with ever more narrowly focused laser beams, needs to be explored. Furthermore, as the size of abrasives decreases their mass and thus kinetic energy reduces as the inverse power of 3, which makes usage of sub-micron grits almost unpractical with current technology. Therefore, ways to energize the abrasive particles, such as ultrasonic cavitation micro-bubbles, thermal heating by pulsed laser, as well as greater operating pressures, will need to be developed in order to process surfaces with lateral dimensions at the micron scale or less.

### *Magnetic Field-Assisted Finishing (MAF)*

Although many research groups have experimentally demonstrated the feasibility of MAF for surface and edge finishing of micro parts, the transition of MAF from the laboratory to practice remains challenging. The practical realization of MAF processes might be hindered by a lack of appropriate MAF process models. Modelling of the MAF process could enable control of the

material removal rate and accurate prediction of surface finish, which would lead to the industrial implementation of MAF processes.

### Modeling of small-scale material removal processes

Several FE and MD simulation works have been done for small-scale material removal process to understand the material removal mechanism and other responses. However, the majority of works is limited to specific cutting conditions or to single grits, which are useful to study the dominated 'size effect' but have less convergence towards real process. Hence, in future, there is a need to develop feasible hybrid models (combining different modelling approaches such as FE-empirical, kinematic-empirical, analytical-kinematic etc.) by integrating the combined action of stochastically distributed grits. The hybrid modeling approach is already proven to be successful for loose abrasive process and needs to be expanded for fixed abrasive processes. Moreover, there is a need to predict the process behaviour with dynamic grit distribution variations (for loose abrasive processes) or rapid grits wear (for the fixed abrasive process).

## 6. Conclusions

This keynote paper gave a comprehensive overview of products and applications that have features on the micro scale. The focus was on features in hard and brittle materials, which are commonly machined via abrasive processes. The paper explored a number of promising systems, devices and tools. Abrasive processes to machine such products and their capabilities were investigated in detail. Particularly in view of the continuing miniaturization of the features, a further miniaturization of the tools and scales of the abrasive processes themselves is required. The review in this keynote paper showed that there is a need for a deeper understanding of the mechanisms of abrasive small scale material removal processes to achieve this. Recommendations on future research directions were given. However, the review also showed that knowledge from common scale abrasive machining is not fully scalable to the micro scale. This was e.g. demonstrated by the scale effects of the brittle-ductile transition area. Modelling of such small scale material removal processes appears to be a promising technique to gain a deeper understanding of the underlying mechanisms.

## References

- [1] Achtsnick M, Drabbe J, Hoogstrate AM, Karpuschewski B (2004) Erosion behaviour and pattern transfer accuracy of protecting masks for micro-abrasive blasting. *J Mater Process Tech* 149(1-3):43-9.
- [2] Aghan RL, McPherson R (1973) Mechanism of Material Removal During Abrasion of Rutile. *J Am Ceram Soc* 56(1):46-7.
- [3] Agrawal PM, Raff LM, Bukkapatnam S, Komanduri R (2010) Molecular dynamics investigations on polishing of a silicon wafer with a diamond abrasive. *Appl Phys A* 100(1):89-104.
- [4] Ajarapu SK (2004) Experimental and Numerical Investigation of Ductile Regime Machining of Silicon Nitride. *AIP Conference Proceedings*. AIP, pp. 1377-1383.
- [5] Arif M, Rahman M, San WY (2012) A state-of-the-art review of ductile cutting of silicon wafers for semiconductor and microelectronics industries. *Int J Adv Manuf Technol* 63(5-8):481-504.
- [6] Arrabiyeh P, Bohley M, Ströer F, Kirsch B, Seewig J, Aurich J (2017) Experimental Analysis for the Use of Sodium Dodecyl Sulfate as a Soluble Metal Cutting Fluid for Micromachining with Electroless-Plated Micropencil Grinding Tools. *Inventions* 2(4):29.
- [7] Arrabiyeh P, Raval V, Kirsch B, Bohley M, Aurich J (2016) Electroless Plating of Micro Pencil Grinding Tools with 5-10  $\mu\text{m}$  Sized cBN Grits. *Adv Mat Res* 1140:133-40.
- [8] Arrabiyeh PA, Kirsch B, Aurich J (2016) Development of Micro Pencil Grinding Tools via an Electroless Plating Process. *Volume 1: Processing*. ASME, V001T02A006.
- [9] Aurich J, Carrella M, Walk M (2015) Micro grinding with ultra small micro pencil grinding tools using an integrated machine tool. *CIRP Annals* 64(1):325-8.

- [10] Aurich J, Engmann J, Schueler GM, Haberland R (2009) Micro grinding tool for manufacture of complex structures in brittle materials. *CIRP Annals* 58(1):311-4.
- [11] Aurich J, Reichenbach IG, Schüler GM (2012) Manufacture and application of ultra-small micro end mills. *CIRP Annals* 61(1):83-6.
- [12] Axinte D, Butler-Smith P, Akgun C, Kolluru K (2013) On the influence of single grit micro-geometry on grinding behavior of ductile and brittle materials. *Int J Mach Tool Manu* 74:12-8.
- [13] Backer WR, Marshall ER, Shaw MC (1952) The size effect in metal cutting. *Trans. ASME* 74:61-71.
- [14] Ball MJ, Murphy NA, Shore P (1992) Electrolytically assisted ductile-mode diamond grinding of BK7 and SF10 optical glasses. in Baker LR, (Ed.). *Commercial Applications of Precision Manufacturing at the Sub-Micron Level*. SPIE, pp. 30-38.
- [15] Ballandras S, Wilm M, Gijs M, Sayah A, Andrey E, Boy J-J, Robert L, Baudouy J-C, Daniau W, Laude V (2001) Periodic arrays of transducers built using sand blasting and ultrasound micromachining techniques for the fabrication of piezocomposite materials. in Yuhua DEE, Schneider SC, (Eds.). *2001 IEEE ultrasonics symposium*. IEEE, pp. 871-874.
- [16] Beaucamp A, Katsuura T, Kawara Z (2017) A novel ultrasonic cavitation assisted fluid jet polishing system. *CIRP Annals* 66(1):301-4.
- [17] Beaucamp A, Namba Y (2013) Super-smooth finishing of diamond turned hard X-ray molding dies by combined fluid jet and bonnet polishing. *CIRP Annals* 62(1):315-8.
- [18] Beaucamp A, Namba Y, Freeman R (2012) Dynamic multiphase modeling and optimization of fluid jet polishing process. *CIRP Annals* 61(1):315-8.
- [19] Beaucamp A, Namba Y, Messelink W, Walker D, Charlton P, Freeman R (2014) Surface Integrity of Fluid Jet Polished Tungsten Carbide. *Procedia CIRP* 13:377-81.
- [20] Belder D, Kohler F, Ludwig M, Tolba K, Piehl N (2006) Coating of powder-blasted channels for high-performance microchip electrophoresis. *Electrophoresis* 27(16):3277-83.
- [21] Belloy E, Pawlowski A-G, Sayah A, Gijs MAM (2002) Microfabrication of high-aspect ratio and complex monolithic structures in glass. *J Microelectromech S* 11(5):521-7.
- [22] Belloy E, Sayah A, Gijs MAM (2000) Powder blasting for three-dimensional microstructuring of glass. *Sensor Actuat A-Phys* 86(3):231-7.
- [23] Belloy E, Sayah A, Gijs MAM (2001) Oblique powder blasting for three-dimensional micromachining of brittle materials. *Sensor Actuat A-Phys* 92(1-3):358-63.
- [24] Bifano TG, Dow TA, Scattergood RO (1991) Ductile-Regime Grinding: A New Technology for Machining Brittle Materials. *J Eng Ind T ASME* 113(2):184.
- [25] Blackley WS, Scattergood RO (1991) Ductile-regime machining model for diamond turning of brittle materials. *Precis Eng* 13(2):95-103.
- [26] Blake PN, Scattergood RO (1990) Ductile-Regime Machining of Germanium and Silicon. *J Am Ceram Soc* 73(4):949-57.
- [27] Bouzakis K-D, Michailidis N, Hadjiyiannis S, Efstathiou K, Pavlidou E, Erkens G, Rambadt S, Wirth I (2001) Improvement of PVD coated inserts cutting performance, through appropriate mechanical treatments of substrate and coating surface. *Surf Coat Tech* 146-147:443-50.
- [28] Bouzakis K-D, Skordaris G, Mirisidis I, Mesomeris G, Michailidis N, Pavlidou E, Erkens G (2005) Micro-blasting of PVD Films, an Effective Way to Increase the Cutting Performance of Coated Cemented Carbide Tools. *CIRP Annals* 54(1):95-8.
- [29] Boy JJ, Andrey E, Boulouize A, Khan-Malek C (2010) Developments in microultrasonic machining (MUSM) at FEMTO-ST. *Int J Adv Manuf Technol* 47(1-4):37-45.
- [30] Bruzzone AAG, Costa HL, Lonardo PM, Lucca DA (2008) Advances in engineered surfaces for functional performance. *CIRP Annals* 57(2):750-69.
- [31] Burzynski T, Papini M (2011) Measurement of the particle spatial and velocity distributions in micro-abrasive jets. *Meas Sci Technol* 22(2):25104.
- [32] Butler-Smith P, Axinte D, Daine M, Kong MC (2014) Mechanisms of surface response to overlapped abrasive grits of controlled shapes and positions: An analysis of ductile and brittle materials. *CIRP Annals* 63(1):321-4.
- [33] Butler-Smith PW, Axinte DA, Daine M (2009) Preferentially oriented diamond micro-arrays: A laser patterning technique and preliminary evaluation of their cutting forces and wear characteristics. *Int J Mach Tool Manu* 49(15):1175-84.
- [34] Butler-Smith PW, Axinte DA, Daine M (2011) Ordered diamond micro-arrays for ultra-precision grinding—An evaluation in Ti-6Al-4V. *Int J Mach Tool Manu* 51(1):54-66.
- [35] Cai MB, Li XP, Rahman M (2007) Study of the temperature and stress in nanoscale ductile mode cutting of silicon using molecular dynamics simulation. *J Mater Process Tech* 192-193:607-12.
- [36] Cai MB, Li XP, Rahman M, Tay AAO (2007) Crack initiation in relation to the tool edge radius and cutting conditions in nanoscale cutting of silicon. *Int J Mach Tool Manu* 47(3-4):562-9.
- [37] Cao XD, Kim BH, Chu CN (2013) Hybrid micromachining of glass using ECDM and micro grinding. *Int J Precis Eng Man* 14(1):5-10.
- [38] Cao Z-C, Cheung CF (2014) Theoretical modelling and analysis of the material removal characteristics in fluid jet polishing. *Int J Mech Sci* 89:158-66.
- [39] Cao Z-C, Cheung CF, Ren M (2016) Modelling and characterization of surface generation in Fluid Jet Polishing. *Precis Eng* 43:406-17.
- [40] Carrella M (2016) Zerspanungsmechanismen beim Mikroschleifen von einkristallinem Silizium, PhD, Kaiserslautern, Germany, TU Kaiserslautern, Institute for Manufacturing Technology and Production Systems.

- [41] Carrella M, Aurich JC (2014) Micromachining of Silicon - Study on the Material Removal Mechanism. *Adv Mat Res* 1018:167-74.
- [42] Chen F, Hao S, Miao X, Yin S, Huang S (2018) Numerical and experimental study on low-pressure abrasive flow polishing of rectangular microgroove. *Powder Technol* 327:215-22.
- [43] Chen R, Di Zhang, Wu Y (2018) Study on the influence of standoff distance on substrate damage under an abrasive water jet process by molecular dynamics simulation. *Friction* 6(2):195-207.
- [44] Chen R, Jiang R, Lei H, Liang M (2013) Material removal mechanism during porous silica cluster impact on crystal silicon substrate studied by molecular dynamics simulation. *Appl Surf Sci* 264:148-56.
- [45] Chen S-T, Jiang Z-H (2015) A force controlled grinding-milling technique for quartz-glass micromachining. *J Mater Process Tech* 216:206-15.
- [46] Chen S-T, Lin S-J (2011) Development of an extremely thin grinding-tool for grinding microgrooves in optical glass. *J Mater Process Tech* 211(10):1581-9.
- [47] Chen S-T, Tsai M-Y, Lai Y-C, Liu C-C (2009) Development of a micro diamond grinding tool by compound process. *J Mater Process Tech* 209(10):4698-703.
- [48] Cheng J, Gong Y, Wang J (2013) Modeling and evaluating of surface roughness prediction in micro-grinding on soda-lime glass considering tool character. *Chin J Mech Eng* 26(6):1091-100.
- [49] Cheng J, Gong YD (2013) Experimental study on ductile-regime micro-grinding character of soda-lime glass with diamond tool. *Int J Adv Manuf Technol* 69(1-4):147-60.
- [50] Cheng J, Gong YD (2014) Experimental study of surface generation and force modeling in micro-grinding of single crystal silicon considering crystallographic effects. *Int J Mach Tool Manu* 77:1-15.
- [51] Cheng J, Wang C, Wen X, Gong Y (2014) Modeling and experimental study on micro-fracture behavior and restraining technology in micro-grinding of glass. *Int J Mach Tool Manu* 85:36-48.
- [52] Cherku S, Sundaram MM, Rajurkar KP (2008) Experimental study of micro ultrasonic machining process.
- [53] Cheung FY, Zhou ZF, Geddam A, Li KY (2008) Cutting edge preparation using magnetic polishing and its influence on the performance of high-speed steel drills. *J Mater Process Tech* 208(1-3):196-204.
- [54] Chiffre L de, Kunzmann H, Peggs GN, Lucca DA (2003) Surfaces in Precision Engineering, Microengineering and Nanotechnology. *CIRP Annals* 52(2):561-77.
- [55] Clark WI, Shih AJ, Hardin CW, Lemaster RL, McSpadden SB (2003) Fixed abrasive diamond wire machining—part I: process monitoring and wire tension force. *Int J Mach Tool Manu* 43(5):523-32.
- [56] Courjal N, Guichardaz B, Ulliac G, Rauch J-Y, Sadani B, Lu H-H, Bernal M-P (2011) High aspect ratio lithium niobate ridge waveguides fabricated by optical grade dicing. *J Phys D Appl Phys* 44(30):305101.
- [57] Cvetković S, Morsbach C, Rissing L (2011) Ultra-precision dicing and wire sawing of silicon carbide (SiC). *Microelectron Eng* 88(8):2500-4.
- [58] Dehmadfar D, Friedman J, Papini M (2012) Laser shadowgraphy measurements of abrasive particle spatial, size and velocity distributions through micro-masks used in abrasive jet micro-machining. *J Mater Process Tech* 212(1):137-49.
- [59] Denkena B, Köhler J, Hahmann D, (Eds.) (2011) *A new approach for the simultaneous grinding of cubic microstructures in brittle-hard materials.*
- [60] Denkena B, Köhler J, Schindler A (2014) Behavior of the magnetic abrasive tool for cutting edge preparation of cemented carbide end mills. *Prod Engineer* 8(5):627-33.
- [61] Denkena B, Köhler J, Wang B (2010) Manufacturing of functional riblet structures by profile grinding. *CIRP Journal of Manufacturing Science and Technology* 3(1):14-26.
- [62] Denkena B, Tönshoff HK (2011) *Spanen: Grundlagen*. 3rd ed. Springer, Berlin.
- [63] Dornfeld D, Min S, Takeuchi Y (2006) Recent Advances in Mechanical Micromachining. *CIRP Annals* 55(2):745-68.
- [64] Eder SJ, Bianchi D, Cihak-Bayr U, Vernes A, Betz G (2014) An analysis method for atomistic abrasion simulations featuring rough surfaces and multiple abrasive particles. *Comput Phys Commun* 185(10):2456-66.
- [65] Egashira K, Masuzawa T (1999) Microultrasonic Machining by the Application of Workpiece Vibration. *CIRP Ann-Manuf Techn* 48(1):131-4.
- [66] Evans CJ, Bryan JB (1999) "Structured", "Textured" or "Engineered" Surfaces. *CIRP Annals* 48(2):541-56.
- [67] Fan JM, Wang CY, Wang J, Luo GS (2007) Effect of Nozzle Type and Abrasive on Machinability in Micro Abrasive Air Jet Machining of Glass. *Key Eng Mat* 359-360:404-8.
- [68] Fang FZ, Venkatesh VC (1998) Diamond Cutting of Silicon with Nanometric Finish. *CIRP Annals* 47(1):45-9.
- [69] Fang FZ, Zhang XD, Weckenmann A, Zhang GX, Evans C (2013) Manufacturing and measurement of freeform optics. *CIRP Annals* 62(2):823-46.
- [70] Fang H, Guo P, Yu J (2006) Dwell function algorithm in fluid jet polishing. *Appl Opt* 45(18):4291.
- [71] Feng J (2010) *Micror grinding of Ceramic Materials*, PhD, Michigan, USA, The University of Michigan, Mechanical Engineering.
- [72] Feng J, Chen P, Ni J (2012) Prediction of surface generation in micror grinding of ceramic materials by coupled trajectory and finite element analysis. *Finite Elem Anal Des* 57:67-80.
- [73] Feng J, Chen P, Ni J (2013) Prediction of grinding force in micror grinding of ceramic materials by cohesive zone-based finite element method. *Int J Adv Manuf Technol* 68(5-8):1039-53.
- [74] Feng J, Kim BS, Shih A, Ni J (2009) Tool wear monitoring for micro-end grinding of ceramic materials. *J Mater Process Tech* 209(11):5110-6.
- [75] Fess E, Ruckman J, Li, Yi ED - Taylor, J., Piscotty, M., and Lindquist, A., (Eds.) (1999) *Contour mode deterministic micror grinding*. Optical Society of America.
- [76] Field JE (1992) *The Properties of natural and synthetic diamond*.
- [77] Fu YQ, Luo JK, Nguyen NT, Walton AJ, Flewitt AJ, Zu XT, Li Y, McHale G, Matthews A, Iborra E, Du H, Milne WI (2017) Advances in piezoelectric thin films for acoustic biosensors, acoustofluidics and lab-on-chip applications. *Prog Mater Sci* 89:31-91.
- [78] Gäbler J, Pleger S (2010) Precision and micro CVD diamond-coated grinding tools. *Int J Mach Tool Manu* 50(4):420-4.
- [79] Gäbler J, Schäfer L, Menze B, Hoffmeister H-W (2003) Micro abrasive pencils with CVD diamond coating. *Diam Relat Mater* 12(3-7):707-10.
- [80] Gao Y, Ge P, Liu T (2016) Experiment study on electroplated diamond wire saw slicing single-crystal silicon. *Mat Sci Semicon Proc* 56:106-14.
- [81] Getu H, Ghobeity A, Spelt JK, Papini M (2007) Abrasive jet micromachining of polymethylmethacrylate. *Wear* 263(7-12):1008-15.
- [82] Getu H, Ghobeity A, Spelt JK, Papini M (2008) Abrasive jet micromachining of acrylic and polycarbonate polymers at oblique angles of attack. *Wear* 265(5-6):888-901.
- [83] Getu H, Spelt JK, Papini M (2008) Cryogenically assisted abrasive jet micromachining of polymers. *J Micromech Microeng* 18(11):115010.
- [84] Ghobeity A, Crabtree HJ, Papini M, Spelt JK (2012) Characterisation and comparison of microfluidic chips formed using abrasive jet micromachining and wet etching. *J Micromech Microeng* 22(2):25014.
- [85] Ghobeity A, Getu H, Krajac T, Spelt JK, Papini M (2007) Process repeatability in abrasive jet micro-machining. *J Mater Process Tech* 190(1-3):51-60.
- [86] Ghobeity A, Krajac T, Burzynski T, Papini M, Spelt JK (2008) Surface evolution models in abrasive jet micromachining. *Wear* 264(3-4):185-98.
- [87] Ghobeity A, Papini M, Spelt JK (2009) Abrasive jet micro-machining of planar areas and transitional slopes in glass using target oscillation. *J Mater Process Tech* 209(11):5123-32.
- [88] Goel S, Luo X, Agrawal A, Reuben RL (2015) Diamond machining of silicon: A review of advances in molecular dynamics simulation. *Int J Mach Tool Manu* 88:131-64.
- [89] Gong YD, Wen XL, Cheng J, Yin GQ, Wang C (2014) Experimental study on fabrication and evaluation of a micro-scale shaft grinding tool. *J Mech Sci Technol* 28(3):1027-37.
- [90] Gorodkova AE, Dyakonov AA, Herreinstein AV (2017) Thermophysical modeling of micror grinding. *Russ Eng Res* 37(7):647-50.
- [91] Gradeen AG, Papini M, Spelt JK (2014) The effect of temperature on the cryogenic abrasive jet micro-machining of polytetrafluoroethylene, high carbon steel and polydimethylsiloxane. *Wear* 317(1-2):170-8.
- [92] Guo J, Suzuki H, Higuchi T (2013) Development of micro polishing system using a magnetostrictive vibrating polisher. *Precis Eng* 37(1):81-7.
- [93] Haghbin N, Ahmadvadeh F, Spelt JK, Papini M (2015) Effect of entrained air in abrasive water jet micro-machining: Reduction of channel width and waviness using slurry entrainment. *Wear* 344-345:99-109.
- [94] Haghbin N, Ahmadvadeh F, Spelt JK, Papini M (2015) High pressure abrasive slurry jet micro-machining using slurry entrainment. *Int J Adv Manuf Technol* 36(2):185.
- [95] Hahn RS (1966) On the Mechanics of the Grinding Process Under Plunge Cut Conditions. *J Eng Ind, T ASME* 88(1):72.
- [96] Haj Mohammad Jafar R, Nouraei H, Emamifar M, Papini M, Spelt JK (2015) Erosion modeling in abrasive slurry jet micro-machining of brittle materials. *J Manuf Process* 17:127-40.
- [97] Haj Mohammad Jafar R, Spelt JK, Papini M (2013) Surface roughness and erosion rate of abrasive jet micro-machined channels: Experiments and analytical model. *Wear* 303(1-2):138-45.
- [98] Haj Mohammad Jafar R, Spelt JK, Papini M (2014) Surface Finishing of Micro-channels Using Low Kinetic Energy Abrasives. *Int J Mech Eng Mechatronics*.
- [99] Han X, Hu Y, Yu S (2009) Investigation of material removal mechanism of silicon wafer in the chemical mechanical polishing process using molecular dynamics simulation method. *Appl Phys A* 95(3):899-905.
- [100] Hashimoto F, Yamaguchi H, Krajnik P, Wegener K, Chaudhari R, Hoffmeister H-W, Kuster F (2016) Abrasive fine-finishing technology. *CIRP Annals* 65(2):597-620.
- [101] Heaney PJ, Sumant AV, Torres CD, Carpick RW, Pfefferkorn FE (2008) Diamond coatings for micro end mills: Enabling the dry machining of aluminum at the micro-scale. *Diam Relat Mater* 17(3):223-33.
- [102] Hoffmeister HW, Wenda A (2000) Novel Grinding Tools for Machining Precision Micro Parts of Hard and Brittle Materials. *ASPE Annual Proceedings 15th Annual Meeting*.
- [103] Horsch C, Schulze V, Löhle D (2006) Deburring and surface conditioning of micro milled structures by micro peening and ultrasonic wet peening. *Microsys Technol* 12(7):691-6.
- [104] <http://www.yole.fr/>.
- [105] Huu Loc P, Shiou F-J, Yu Z-R, Hsu W-Y (2013) Investigation of Optimal Air-Driving Fluid Jet Polishing Parameters for the Surface Finish of N-BK7 Optical Glass. *J Manuf Sci E, T ASME* 135(1):11015.
- [106] Imanaka A, Fujino S, Maneta S (1972) Direct observation of material removal process during grinding of ceramics by micro-flash- technique. *The science of ceramic machining and surface finishing XI* 348:37-43.
- [107] Ivantsiv V, Spelt JK, Papini M (2009) Mass flow rate measurement in abrasive jets using acoustic emission. *Meas Sci Technol* 20(9):95402.
- [108] Jafar RHM, Papini M, Spelt JK (2013) Simulation of erosive smoothing in the abrasive jet micro-machining of glass. *J Mater Process Tech* 213(12):2254-61.
- [109] Jain AK, Pandey PM (2016) Experimental studies on tool wear in  $\mu$ -RUM process. *Int J Adv Manuf Technol* 85(9-12):2125-38.

- [110] Jain VK, Kalia S, Sidpara AM (2012) Some aspects of fabrication of micro devices by electrochemical micromachining (ECMM) and its finishing by magnetorheological fluid. *Int J Adv Manuf Technol* 59(9-12):987-96.
- [111] James S, Sundaram MM (2013) A molecular dynamics study of the effect of impact velocity, particle size and angle of impact of abrasive grain in the Vibration Assisted Nano Impact-machining by Loose Abrasives. *Wear* 303(1-2):510-8.
- [112] Jang K-I, Kim D-Y, Maeng S, Lee W, Han J, Seok J, Je T-J, Kang S, Min B-K (2012) Deburring microparts using a magnetorheological fluid. *Int J Mach Tool Manu* 53(1):170-5.
- [113] Judal KB, Yadava V (2013) Modeling and simulation of cylindrical electrochemical magnetic abrasive machining of AISI-420 magnetic steel. *J Mater Process Tech* 213(12):2089-100.
- [114] Kai E, Takahisa M, Masatoshi F, Xi, Qing, Sun. (1997) Application of USM to Micromachining by On-the-machine Tool Fabrication. *Int J Electr Mach* 2(0):31-6.
- [115] Kang J, Yamaguchi H (2012) Internal finishing of capillary tubes by magnetic abrasive finishing using a multiple pole-tip system. *Precis Eng* 36(3):510-6.
- [116] Kannappan S, Malkin S (1972) Effects of Grain Size and Operating Parameters on the Mechanics of Grinding. *J Eng Ind, T ASME* 94(3):833.
- [117] Kassen G (1969) Simulation des Schleifprozesses. *Industrie-Anzeiger* 91(24):29-32.
- [118] Katahira K, Ohmori H, Uehara Y, Watanabe Y, Lin W, Suzuki T (2002) Study on ELID ground micro-tool and its applications. *IEEE ICIT '02*. IEEE, pp. 1138-1141.
- [119] Katahira K, Ohmori H, Uehara Y, Watanabe Y, Lin WM, Komotori J, Mizutani M (2004) Fabrication of High-Quality Surfaces on Micro Tools by the ELID Grinding Technique. *Key Eng Mat* 257-258:441-6.
- [120] Kirsch B, Aurich JC (2016) Herstellung von mikrostrukturierten Oberflächen mit einer Spezialschleifscheibe und Analyse des Abtragverhaltens. *Jahrbuch Schleifen, Honen, Läppen und Polieren - Verfahren und Maschinen* 67:12-27.
- [121] Kleinstreuer C (2013) *Microfluidics and Nanofluidics*. John Wiley & Sons, Inc, Hoboken, NJ, USA.
- [122] Klocke F, Gorgels C, Bouzakis E, Stuckenberg A (2009) Tool life increase of coated carbide tools by micro blasting. *Prod Engineer* 3(4-5):453-9.
- [123] Kohlheyer D, Eijkel JCT, Schlautmann S, van den Berg A, Schasfoort RBM (2008) Bubble-free operation of a microfluidic free-flow electrophoresis chip with integrated Pt electrodes. *Anal Chem* 80(11):4111-8.
- [124] König W, Cronjäger L, Spur G, Tönshoff HK, Vigneau M, Zdeblick WJ (1990) Machining of New Materials. *CIRP Annals* 39(2):673-81.
- [125] Kowsari K, James DF, Papini M, Spelt JK (2014) The effects of dilute polymer solution elasticity and viscosity on abrasive slurry jet micro-machining of glass. *Wear* 309(1-2):112-9.
- [126] Kowsari K, Nouhi A, Hadavi V, Spelt JK, Papini M (2017) Prediction of the erosive footprint in the abrasive jet micro-machining of flat and curved glass. *Tribol Int* 106:101-8.
- [127] Kowsari K, Nouraei H, James DF, Spelt JK, Papini M (2014) Abrasive slurry jet micro-machining of holes in brittle and ductile materials. *J Mater Process Tech* 214(9):1909-20.
- [128] Kowsari K, Sookhakilari MR, Nouraei H, Papini M, Spelt JK (2016) Hybrid erosive jet micro-milling of sintered ceramic wafers with and without copper-filled through-holes. *J Mater Process Tech* 230:198-210.
- [129] Lacharme F, Gijns MAM (2006) Pressure injection in continuous sample flow electrophoresis microchips. *Sensor Actuat B-Chem* 117(2):384-90.
- [130] Lawn BR, Evans AG (1977) A model for crack initiation in elastic/plastic indentation fields. *J Mater Sci* 12(11):2195-9.
- [131] Lee P-H, Lee SW (2011) Experimental characterization of micro-grinding process using compressed chilly air. *Int J Mach Tool Manu* 51(3):201-9.
- [132] Lee SB, Tani Y, Enomoto T, Sato H (2005) Development of a Dicing Blade With Photopolymerizable Resins for Improving Machinability. *CIRP Annals* 54(1):293-6.
- [133] Lee S-J, Sundararajan N (op. 2010) *Microfabrication for microfluidics*. Artech House, Boston, London.
- [134] Lee SW, Choi HJ, Lee HW, Choi JY, Jeong HD (2003) A Study of Micro-Tool Machining Using Electrolytic In-Process Dressing and an Evaluation of its Characteristics. *Key Eng Mat* 238-239:35-42.
- [135] Li B, Ding Z, Xiao J, Liang SY (2016) Maraging steel 3J33 phase transformation during micro-grinding. *Mater Lett* 164:217-20.
- [136] Li J, Geng D, Zhang D, Qin W, Jiang Y (2018) Ultrasonic vibration mill-grinding of single-crystal silicon carbide for pressure sensor diaphragms. *Ceram Int* 44(3):3107-12.
- [137] Li K-M, Lin C-P (2012) Study on minimum quantity lubrication in micro-grinding. *Int J Adv Manuf Technol* 62(1-4):99-105.
- [138] Liao YS, Chen LC (2009) A method of etching and powder blasting for microholes on brittle materials. *J Mater Process Tech* 209(9):4390-4.
- [139] Lin J-W, Cheng M-H (2014) Investigation of chipping and wear of silicon wafer dicing. *J Manuf Process* 16(3):373-8.
- [140] Liu K, Li X, Liang SY (2004) Nanometer-Scale Ductile Cutting of Tungsten Carbide. *J Manuf Process* 6(2):187-95.
- [141] Liu K, Li XP, Liang SY (2007) The mechanism of ductile chip formation in cutting of brittle materials. *Int J Adv Manuf Technol* 33(9-10):875-84.
- [142] Liu Z, Nouraei H, Papini M, Spelt JK (2014) Abrasive enhanced electrochemical slurry jet micro-machining: Comparative experiments and synergistic effects. *J Mater Process Tech* 214(9):1886-94.
- [143] Liu Z, Nouraei H, Spelt JK, Papini M (2015) Electrochemical slurry jet micro-machining of tungsten carbide with a sodium chloride solution. *Precis Eng* 40:189-98.
- [144] Lomas T, Wisitsoraat A, Chevasuvit F, Tuantranont A (2009) A precision hot embossing mold fabricated by high-resolution powder blasting with polydimethylsiloxane and SU-8 masking technology. *J Micromech Microeng* 19(3):35002.
- [145] Lomdahl GS, McPherson R (1981) A scale effect in the abrasive wear of glass. *Wear* 73(1):205-8.
- [146] Lozano Torrubia P, Axinte DA, Billingham J (2015) Stochastic modelling of abrasive waterjet footprints using finite element analysis. *Int J Mach Tool Manu* 95:39-51.
- [147] Luan Q, Tan Y, Akhmadaliev S, Zhou S, Yu H, Zhang H, Chen F (2015) Optical ridge waveguides in Nd: CNGG disorder laser crystal produced by combination of carbon ion irradiation and precise diamond blade dicing. *Opt Mater* 39:247-50.
- [148] Luo SY, Wang ZW (2008) Studies of chipping mechanisms for dicing silicon wafers. *Int J Adv Manuf Technol* 35(11-12):1206-18.
- [149] Malkin S (1976) Selection of Operating Parameters in Surface Grinding of Steels. *J Eng Ind, T ASME* 98(1):56.
- [150] Malkin S, (1981). Grinding mechanisms for metallic and nonmetallic materials. *Ninth North American Manufacturing*, pp. 235-239.
- [151] Malkin S, Ritter JE (1989) Grinding Mechanisms and Strength Degradation for Ceramics. *J Eng Ind, T ASME* 111(2):167.
- [152] Malshe A, Rajurkar K, Samant A, Hansen HN, Bapat S, Jiang W (2013) Bio-inspired functional surfaces for advanced applications. *CIRP Annals* 62(2):607-28.
- [153] Malshe AP, Bapat S, Rajurkar KP, Haitjema H (2018) Bio-inspired textures for functional applications. *CIRP Annals* 67(2):627-50.
- [154] Markopoulos AP, Savvopoulos IK, Karkalos NE, Manolakis DE (2015) Molecular dynamics modeling of a single diamond abrasive grain in grinding. *Front Mech Eng* 10(2):168-75.
- [155] Marshall DB, Lawn BR (1986) Indentation of Brittle Materials. in Blau PJ, Lawn BR, (Eds.). *Microindentation techniques in materials science and engineering*. International Metallographic Society. Philadelphia, PA, 26-46.
- [156] Mathai G, Melkote S (2012) Effect of process parameters on the rate of abrasive assisted brush deburring of microgrooves. *Int J Mach Tool Manu* 57:46-54.
- [157] Mathai G, Melkote S, Rosen D (2013) Material removal during abrasive impregnated brush deburring of micromilled grooves in NiTi foils. *Int J Mach Tool Manu* 72:37-49.
- [158] Matsumaru K, Takata A, Ishizaki K (2005) Advanced thin dicing blade for sapphire substrate. *Sci Technol Adv Mat* 6(2):120-2.
- [159] Matsumura T, Konno T, Tobe S, Komatsu T (2011) Deburring of Micro-Scale Structures Machined in Milling. *Proceedings of the ASME international manufacturing science and engineering conference 2010*. ASME. New York, pp. 105-112.
- [160] Matsumura T, Muramatsu T, Fueki S (2011) Abrasive water jet machining of glass with stagnation effect. *CIRP Annals* 60(1):355-8.
- [161] Matsuzawa T, Ohmori H, Zhang C, Li W, Yamagata Y, Moriyasu S, Makinouchi A (2001) Micro-Spherical Lens Mold Fabrication by Cup-Type Metal-Bond Grinding Wheels Applying ELID (Electrolytic In-Process Dressing). *Key Eng Mat* 196:167-76.
- [162] McKeown PA, Carlisle K, Shore P, Read RF (1990) Ultraprecision, high stiffness CNC grinding machines for ductile mode grinding of brittle materials. in Lettington AH, (Ed.). *Infrared Technology and Applications*. SPIE, p. 301.
- [163] Messelink WACM, Waeger R, Wons T, Meeder M, Heiniger KC, Faehle OW (2005) Prepolishing and finishing of optical surfaces using fluid jet polishing. in Stahl HP, (Ed.). *Optical Manufacturing and Testing VI*. SPIE, p. 586908.
- [164] Miller DS (2003) Developments in abrasive waterjets for micromachining. *Proceedings of 2003 WJTA American Waterjet Conference*.
- [165] Mineta T, Takada T, Makino E, Kawashima T, Shibata T (2009) A wet abrasive blasting process for smooth micromachining of glass by ductile-mode removal. *J Micromech Microeng* 19(1):15031.
- [166] Misri I, Hareesh P, Yang S, DeVoe DL (2012) Microfabrication of bulk PZT transducers by dry film photolithography and micro powder blasting. *J Micromech Microeng* 22(8):85017.
- [167] Mohr O (1900) Welche Umstände bedingen die Elastizitätsgrenze und den Bruch eines Materials? *Zeitschrift des Vereins deutscher Ingenieure* 44(45):1524-1530.
- [168] Morgan C, Ryan Vallance R, R. Marsh E (2005) Micro Grinding Blind Holes in Hard Tungsten Carbide with Polycrystalline Diamond Micro Tools. *20th Annual Meeting of the American Society for Precision Engineering, ASPE 2005*.
- [169] Morgan CJ, Vallance RR, Marsh ER (2007) Specific grinding energy while microgrinding tungsten carbide with polycrystalline diamond micro tools. *ICOMM-2007 2nd International Conference on Micro-Manufacturing*:180-7.
- [170] Nakasuji T, Kodera S, Hara S, Matsunaga H, Ikawa N, Shimada S (1990) Diamond Turning of Brittle Materials for Optical Components. *CIRP Annals* 39(1):89-92.
- [171] Namba Y, Yamada Y, Tsuboi A, Unno K, Nakao H, Inasaki I (1992) Surface Structure of Mn-Zn Ferrite Single Crystals Ground by an Ultraprecision Surface Grinder with Various Diamond Wheels. *CIRP Annals* 41(1):347-51.
- [172] Nouhi A, Sookhak Lari MR, Spelt JK, Papini M (2015) Implementation of a shadow mask for direct writing in abrasive jet micro-machining. *J Mater Process Tech* 223:232-9.
- [173] Nouraei H, Kowsari K, Papini M, Spelt JK (2016) Operating parameters to minimize feature size in abrasive slurry jet micro-machining. *Precis Eng* 44:109-23.
- [174] Nouraei H, Kowsari K, Spelt JK, Papini M (2014) Surface evolution models for abrasive slurry jet micro-machining of channels and holes in glass. *Wear* 309(1-2):65-73.

- [175] Nouraei H, Wodoslawsky A, Papini M, Spelt JK (2013) Characteristics of abrasive slurry jet micro-machining: A comparison with abrasive air jet micro-machining. *J Mater Process Tech* 213(10):1711–24.
- [176] Nteziyaremye V, Wang Y, Li W, Shih A, Yamaguchi H (2014) Surface Finishing of Needles for High-performance Biopsy. *Procedia CIRP* 14:48–53.
- [177] Ohmori H Electrolytic In-Process Dressing (ELID) Technologies: Fundamentals and Applications.
- [178] Ohmori H, Katahira K, Naruse T, Uehara Y, Nakao A, Mizutani M (2007) Microscopic Grinding Effects on Fabrication of Ultra-fine Micro Tools. *CIRP Annals* 56(1):569–72.
- [179] Ohmori H, Katahira K, Uehara Y, Watanabe Y, Lin W (2003) Improvement of Mechanical Strength of Micro Tools by Controlling Surface Characteristics. *CIRP Annals* 52(1):467–70.
- [180] Oliveira JFG, Bottene AC, França TV (2010) A novel dressing technique for texturing of ground surfaces. *CIRP Annals* 59(1):361–4.
- [181] Onikura H, Inoue R, Okuno K, Ohnishi O (2003) Fabrication of Electroplated Micro Grinding Wheels and Manufacturing of Microstructures with Ultrasonic Vibration. *Key Eng Mat* 238-239:9–14.
- [182] Onikura H, Ohnishi O, Take Y, Kobayashi A (2000) Fabrication of Micro Carbide Tools by Ultrasonic Vibration Grinding. *CIRP Annals* 49(1):257–60.
- [183] Ota M, Miyahara K (1990) Influence of grinding on flexural strength of ceramics. *SME 4th International Grinding Conference*:90–538.
- [184] Pacella M, Axinte DA, Butler-Smith PW, Shipway P, Daine M, Wort C (2016) An Assessment of the Wear Characteristics of Microcutting Arrays Produced From Polycrystalline Diamond and Cubic Boron Nitride Composites. *J Manuf Sci E\_T ASME* 138(2):21001.
- [185] Park DS, Seo TI, Cho MW (2005) Mechanical etching of micro pockets by powder blasting. *Int J Adv Manuf Technol* 25(11-12):1098–104.
- [186] Park H-K, Onikura H, Ohnishi O, Sharifuddin A (2010) Development of micro-diamond tools through electroless composite plating and investigation into micro-machining characteristics. *Precis Eng* 34(3):376–86.
- [187] Park HW, Liang SY (2008) Force modeling of micro-grinding incorporating crystallographic effects. *Int J Mach Tool Manu* 48(15):1658–67.
- [188] Pawlowski A-G, Belloy E, Sayah A, Gijs MAM (2003) Powder blasting patterning technology for microfabrication of complex suspended structures in glass. *Microelectron Eng* 67-68:557–65.
- [189] Pu Q-S, Lutttge R, Gardeniers HJGE, van den Berg A (2003) Comparison of capillary zone electrophoresis performance of powder-blasted and hydrogen fluoride-etched microchannels in glass. *Electrophoresis* 24(1-2):162–71.
- [190] Qi H, Wen D, Lu C, Li G (2016) Numerical and experimental study on ultrasonic vibration-assisted micro-channelling of glasses using an abrasive slurry jet. *Int J Mech Sci* 110:94–107.
- [191] Quan J, Fang Q, Chen J, Xie C, Liu Y, Wen P (2017) Investigation of subsurface damage considering the abrasive particle rotation in brittle material grinding. *Int J Adv Manuf Technol* 90(9-12):2461–76.
- [192] Ramesh K, Huang H, Yin L, Zhao J (2004) Microgrinding of deep micro grooves with high table reversal speed. *Int J Mach Tool Manu* 44(1):39–49.
- [193] Ramsden JJ, Allen DM, Stephenson DJ, Alcock JR, Peggs GN, Fuller G, Goch G (2007) The Design and Manufacture of Biomedical Surfaces. *CIRP Annals* 56(2):687–711.
- [194] Riveros RE, Hann JN, Taylor CR, Yamaguchi H (2013) Nanoscale Surface Modifications by Magnetic Field-Assisted Finishing. *J Manuf Sci E\_T ASME* 135(5):51014.
- [195] Riveros RE, Yamaguchi H, Boggs T, Mitsuishi I, Mitsuda K, Takagi U, Ezoe Y, Ishizu K, Moriyama T (2012) Magnetic Field-Assisted Finishing of Silicon Microelectromechanical Systems Micropore X-Ray Optics. *J Manuf Sci E\_T ASME* 134(5):51001.
- [196] Riveros RE, Yamaguchi H, Mitsuishi I, Takagi U, Ezoe Y, Kato F, Sugiyama S, Yamasaki N, Mitsuda K (2010) Development of an alternating magnetic-field-assisted finishing process for microelectromechanical systems micropore x-ray optics. *Appl Opt* 49(18):3511–21.
- [197] S, B, Toh., R M, (Eds.) (1984) *Fine scale abrasive wear of ceramics by a plastic cutting process*.
- [198] Sarwade A, Sundaram MM, Rajurkar KP (2010) Investigation of micro hole drilling in bovine rib using micro rotary ultrasonic machining. Shanghai Jiaotong University Press, pp. 411–416.
- [199] Sarwade A, Sundaram MM, Rajurkar KP (2010) Micro rotary ultrasonic machining: Effect of machining parameters on material removal rate, pp. 113–120.
- [200] Sayah A, Gijs MAM (2015) Simulation and Fabrication of a Three-dimensional Microfluidic Mixer in a Monolithic Glass Substrate. *Procedia Engineer* 120:229–32.
- [201] Sayah A, Parashar VK, Pawlowski A-G, Gijs MAM (2005) Elastomer mask for powder blasting microfabrication. *Sensor Actuat A-Phys* 125(1):84–90.
- [202] Sayah A, Solignac D, Cueni T, Gijs MAM (2000) Development of novel low temperature bonding technologies for microchip chemical analysis applications. *Sensor Actuat A-Phys* 84(1-2):103–8.
- [203] Sayah A, Thivolle P-A, Parashar VK, Gijs MAM (2009) Fabrication of microfluidic mixers with varying topography in glass using the powder-blasting process. *J Micromech Microeng* 19(8):85024.
- [204] Schinker MG, Doll W (1987) Turning Of Optical Glasses At Room Temperature. in Langenbeck P, (Ed.). *In-Process Optical Metrology for Precision Machining*. SPIE, p. 70.
- [205] Schlautmann S, Wensink H, Schasfoort R, Elwenspoek M, van den Berg A (2001) Powder-blasting technology as an alternative tool for microfabrication of capillary electrophoresis chips with integrated conductivity sensors. *J Micromech Microeng* 11(4):386–9.
- [206] Setti D, Kirsch B, Arrabiye PA, Aurich JC Visualization of Geometrical Deviations in Micro Grinding by Kinematic Simulations. *ASME 2018 13th International Manufacturing Science and Engineering Conference*, V004T03A038.
- [207] Setti D, Kirsch B, Aurich JC (2017) An Analytical Method for Prediction of Material Deformation Behavior in Grinding Using Single Grit Analogy. *Procedia CIRP* 58:263–8.
- [208] Shen M, Gijs MAM (2009) *TRANSDUCERS 2009: International Solid-State Sensors, Actuators and Microsystems Conference, 2009 ; 21 - 25 June 2009, Denver, Colorado, USA*. IEEE, Piscataway, NJ.
- [209] Shiou F-J, Asmare A (2015) Parameters optimization on surface roughness improvement of Zerodur optical glass using an innovative rotary abrasive fluid multi-jet polishing process. *Precis Eng* 42:93–100.
- [210] Shore P (1990) State of the art in 'damage-free' grinding of advanced engineering ceramics. *Brit Cer Pr* 46:189–200.
- [211] Si L, Guo D, Luo J, Xie G (2012) Planarization process of single crystalline silicon asperity under abrasive rolling effect studied by molecular dynamics simulation. *Appl Phys A* 109(1):119–26.
- [212] Silva EJ, Kirsch B, Bottene AC, Simon A, Aurich JC, Oliveira JFG (2017) Manufacturing of structured surfaces via grinding. *J Mater Process Tech* 243:170–83.
- [213] Silva EJD, Oliveira JFGd, Salles BB, Cardoso RS, Reis VRA (2013) Strategies for production of parts textured by grinding using patterned wheels. *CIRP Annals* 62(1):355–8.
- [214] Solignac D, Gijs MAM (2003) Pressure Pulse Injection: A Powerful Alternative to Electrokinetic Sample Loading in Electrophoresis Microchips. *Anal Chem* 75(7):1652–7.
- [215] Sookhak Lari MR, Papini M (2016) Inverse methods to gradient etch three-dimensional features with prescribed topographies using abrasive jet micro-machining: Part I – Modeling. *Precis Eng* 45:272–84.
- [216] Sookhak Lari MR, Teti M, Papini M (2016) Inverse methods to gradient etch three-dimensional features with prescribed topographies using abrasive jet micro-machining: Part II—Verification with micro-machining experiments. *Precis Eng* 45:262–71.
- [217] Stepień P (2007) Grinding forces in regular surface texture generation. *Int J Mach Tool Manu* 47(14):2098–110.
- [218] Sundaram MM, Sarwade A, Rachuri K, Rajurkar KP (2009) Micro rotary ultrasonic machining, pp. 621–628.
- [219] Suzuki H, Hamada S, Okino T, Kondo M, Yamagata Y, Higuchi T (2010) Ultraprecision finishing of micro-aspheric surface by ultrasonic two-axis vibration assisted polishing. *CIRP Annals* 59(1):347–50.
- [220] Suzuki H, Kamano T, Higuchi T, Tanioka T, Shimamura K, Yokoyama M, Kitajima T, Okuyama S (2001) Precision Glass Molding of Micro Fresnel Lens. Experimental Study on Molding Characteristics with Molding Conditions and Feasibility Study. *J Jpn Precis Eng* 67(3):438–43.
- [221] Suzuki H, Moriwaki T, Okino T, Ando Y (2006) Development of Ultrasonic Vibration Assisted Polishing Machine for Micro Aspheric Die and Mold. *CIRP Annals* 55(1):385–8.
- [222] Takenaka N (1966) A study on the grinding action by single grit. *Annals of the CIRP* 13(1):183–90.
- [223] Tanaka H, Shimada S, Anthony L (2007) Requirements for Ductile-mode Machining Based on Deformation Analysis of Mono-crystalline Silicon by Molecular Dynamics Simulation. *CIRP Annals* 56(1):53–6.
- [224] Tönshoff HK, Karpuschewski B, Mohlfeld A, Seegers H (1998) Influence of stress distribution on adhesion strength of sputtered hard coatings. *Thin Solid Films* 332(1-2):146–50.
- [225] Tönshoff HK, Karpuschewski B, Mohlfeld A, Seegers H (1999) Influence of subsurface properties on the adhesion strength of sputtered hard coatings. *Surf Coat Tech* 116-119:524–9.
- [226] Tönshoff HK, Mohlfeld A (1998) Surface treatment of cutting tool substrates. *Int J Mach Tool Manu* 38(5-6):469–76.
- [227] Tricard M, Kordonski WI, Shorey AB, Evans C (2006) Magnetorheological Jet Finishing of Conformal, Freeform and Steep Concave Optics. *CIRP Annals* 55(1):309–12.
- [228] Tsai M-Y, Chen S-T, Liao Y-S, Sung J (2009) Novel diamond conditioner dressing characteristics of CMP polishing pad. *Int J Mach Tool Manu* 49(9):722–9.
- [229] Ueda K, Sugita T, Hiraga H, Iwata K (1991) A J-Integral Approach to Material Removal Mechanisms in Microcutting of Ceramics. *CIRP Annals* 40(1):61–4.
- [230] Umehara N, Mizuguchi S, Kato K, Nakamura S (1993) Microsurface finishing of borosilicate glass with magnetic fluid grinding. *J Magn Magn Mater* 122(1-3):432–6.
- [231] van den Berg A, Olthuis W, Bergveld P, Schasfoort R, Guijt-van Duijn R, Schlautmann S, Frank H, Billiet H, van Dedem G, (Eds.) (2000) *Miniaturized Capillary Electrophoresis System with Integrated Conductivity Detector: Micro Total Analysis Systems 2000*. Springer Netherlands.
- [232] Veenstra TT, Berenschot JW, Gardeniers JGE, Sanders RGP, Elwenspoek MC, van den Berg A (2001) Use of Selective Anodic Bonding to Create Micropump Chambers with Virtually No Dead Volume. *J Electrochem Soc* 148(2):G68.
- [233] Venkatachalam S, Li X, Liang SY (2009) Predictive modeling of transition undeformed chip thickness in ductile-regime micro-machining of single crystal brittle materials. *J Mater Process Tech* 209(7):3306–19.
- [234] W BM, K HL (1995) Crystal morphology identification of diamond and ABN. *Ind Diam Rev* 55(564):11–4.



- [235] Wakuda M, Yamauchi Y, Kanzaki S (2002) Effect of workpiece properties on machinability in abrasive jet machining of ceramic materials. *Precis Eng* 26(2):193-8.
- [236] Walk M, Aurich JC, Engmann J, Schueler GM (2010) Micro-EDM-device for machining tungsten carbide in a desktop machine tool. *10th International Conference of the European Society for Precision Engineering & Nanotechnology* 1:324-7.
- [237] Walk M, Carrella M, Engmann J, Schueler GM, Aurich JC (2011) Micro Pencil Grinding Tools - Manufacturing, Application, and Results. *11th International Conference of the European Society for Precision Engineering & Nanotechnology* 2:260-4.
- [238] Wang AC, Yan BH, Li XT, Huang FY (2002) Use of micro ultrasonic vibration lapping to enhance the precision of microholes drilled by micro electro-discharge machining. *Int J Mach Tool Manu* 42(8):915-23.
- [239] Wang C, Chen J, Fang Q, Liu F, Liu Y (2016) Study on brittle material removal in the grinding process utilizing theoretical analysis and numerical simulation. *Int J Adv Manuf Technol* 87(9-12):2603-14.
- [240] Wang CJ, Cheung CF, Ho LT, Liu MY, Lee WB (2017) A novel multi-jet polishing process and tool for high-efficiency polishing. *Int J Mach Tool Manu* 115:60-73.
- [241] Wang J, Shimada K, Mizutani M, Kuriyagawa T (2018) Effects of abrasive material and particle shape on machining performance in micro ultrasonic machining. *Precis Eng* 51:373-87.
- [242] Wang J-J, Liao Y-Y (2008) Critical Depth of Cut and Specific Cutting Energy of a Microscribing Process for Hard and Brittle Materials. *J Eng Mater\_T ASME* 130(1):11002.
- [243] Wang S, Liu J, Zhang L (2013) Analysis of process parameters of micro fluid-jet polishing on the processing effect. in Chang B, Guo H, (Eds.). SPIE, p. 891205.
- [244] Wang W, Liu ZX, Zhang W, Huang YH, Allen DM (2011) Abrasive electrochemical multi-wire slicing of solar silicon ingots into wafers. *CIRP Annals* 60(1):255-8.
- [245] Wei C, Hu D, Xu K, Ni J (2011) Electrochemical discharge dressing of metal bond micro-grinding tools. *Int J Mach Tool Manu* 51(2):165-8.
- [246] Wensink H (2002) Fabrication of microstructures by powder blasting, Ph.D. thesis, Enschede, University of Twente.
- [247] Wensink H, Elwenspoek MC (2002) A closer look at the ductile-brittle transition in solid particle erosion. *Wear* 253(9-10):1035-43.
- [248] Wensink H, Jansen HV, Berenschot JW, Elwenspoek MC (2000) Mask materials for powder blasting. *J Micromech Microeng* 10(2):175-80.
- [249] Wills-Moren WJ, Read RFJ (1988) Experiences in the precision machining of brittle materials. *Ultraprecision in manufacturing engineering*:3-21.
- [250] Witzendorff P von, Stompe M, Moalem A, Cvetkovic S, Suttmann O, Overmeyer L, Rissing L (2014) Dicing of hard and brittle materials with on-machine laser-dressed metal-bonded diamond blades. *Precis Eng* 38(1):162-7.
- [251] Wu H, Huang H, Jiang F, Xu X (2016) Mechanical wear of different crystallographic orientations for single abrasive diamond scratching on Ta12W. *Int J Refract Met H* 54:260-9.
- [252] Xiao G, To S, Zhang G (2015) Molecular dynamics modelling of brittle-ductile cutting mode transition: Case study on silicon carbide. *Int J Mach Tool Manu* 88:214-22.
- [253] Xie J, Li YH, Yang LF (2015) Study on 5-axial milling on microstructured freeform surface using the macro-ball cutter patterned with micro-cutting-edge array. *CIRP Annals* 64(1):101-4.
- [254] Xie J, Luo MJ, Wu KK, Yang LF, Li DH (2013) Experimental study on cutting temperature and cutting force in dry turning of titanium alloy using a non-coated micro-grooved tool. *Int J Mach Tool Manu* 73:25-36.
- [255] Xu S, Kuriyagawa T, Shimada K, Mizutani M (2017) Recent advances in ultrasonic-assisted machining for the fabrication of micro/nano-textured surfaces. *Front Mech Eng* 12(1):33-45.
- [256] Xu SL, Nishikawa C, Shimada K, Mizutani M, Kuriyagawa T (2013) Surface Textures Fabrication on Zirconia Ceramics by 3D Ultrasonic Vibration Assisted Slant Feed Grinding. *Adv Mat Res* 797:326-31.
- [257] Xu W, Wu Y (2018) A novel approach to fabricate high aspect ratio micro-rod using ultrasonic vibration-assisted centreless grinding. *Int J Mech Sci* 141:21-30.
- [258] Yagyu H, Hayashi S, Tabata O (2004) Application of Nanoparticles Dispersed Polymer to Micropowder Blasting Mask. *J Microelectromech S* 13(1):1-6.
- [259] Yagyu H, Sugano K, Hayashi S, Tabata O (2005) Micropowder blasting with nanoparticles dispersed polymer mask for rapid prototyping of glass chip. *J Micromech Microeng* 15(6):1236-41.
- [260] Yamaguchi H, Kang J (2010) Study of Internal Deburring of Capillary Tubes with Multiple Laser-machined Slits. in Aurich JC, Dornfeld D, (Eds.). *Burrs - Analysis, Control and Removal*. Springer Berlin Heidelberg. Berlin, Heidelberg, pp. 205-212.
- [261] Yamaguchi H, Shinmura T, Ikeda R (2007) Study of Internal Finishing of Austenitic Stainless Steel Capillary Tubes by Magnetic Abrasive Finishing. *J Manuf Sci E\_T ASME* 129(5):885.
- [262] Yamahata C, Chastellain M, Parashar VK, Petri A, Hofmann H, Gijs MAM (2005) Plastic micropump with ferrofluidic actuation. *J Microelectromech S* 14(1):96-102.
- [263] Yamahata C, Gijs MAM (2004) Plastic micropumps using ferrofluid and magnetic membrane actuation. *The 17th IEEE international conference on Micro electro mechanical systems*. IEEE, pp. 458-461.
- [264] Yamahata C, Lacharme F, Burri Y, Gijs MAM (2005) A ball valve micropump in glass fabricated by powder blasting. *Sensor Actuat B-Chem* 110(1):1-7.
- [265] Yamahata C, Lacharme F, Gijs MAM (2005) Glass valveless micropump using electromagnetic actuation. *Microelectron Eng* 78-79:132-7.
- [266] Yamahata C, Lacharme F, Matter J, Schnydrig S, Burri Y, Gijs MAM (2005) Electromagnetically actuated ball valve micropumps. *Transducers '05: Digest of technical papers*. IEEE, pp. 192-196.
- [267] Yamahata C, Lotto C, Al-Assaf E, Gijs MAM (2005) A PMMA valveless micropump using electromagnetic actuation. *Microfluid Nanofluid* 1(3):197-207.
- [268] Yamamoto Y, Suzuki H, Okino T, Hijikata Y, Moriwaki T, Fukuta M, Nishioka M, Kojima Y (2004) Ultra precision grinding of micro aspherical surface - development of a three-axes controlled single point inclined grinding method. *Proc ASPE Ann Meet*:558-61.
- [269] Yan J, Tan T-H (2015) Sintered diamond as a hybrid EDM and grinding tool for the micromachining of single-crystal SiC. *CIRP Annals* 64(1):221-4.
- [270] Yan J, Yoshino M, Kuriagawa T, Shirakashi T, Syoji K, Komanduri R (2001) On the ductile machining of silicon for micro electro-mechanical systems (MEMS), opto-electronic and optical applications. *Mater Sci Eng A* 297(1-2):230-4.
- [271] Yoshino Y (2009) Piezoelectric thin films and their applications for electronics. *J Appl Phys* 105(6):61623.
- [272] Yu Z, Hu X, Rajurkar KP (2006) Influence of Debris Accumulation on Material Removal and Surface Roughness in Micro Ultrasonic Machining of Silicon. *CIRP Annals* 55(1):201-4.
- [273] Yu Z, Ma C, An C, Li J, Guo D (2012) Prediction of tool wear in micro USM. *CIRP Annals* 61(1):227-30.
- [274] Yun DJ, Seo TI, Park DS (2008) Fabrication of Biochips with Micro Fluidic Channels by Micro End-milling and Powder Blasting. *Sensors (Basel, Switzerland)* 8(2):1308-20.
- [275] Zhang L, Kuriyagawa T, Yasutomi Y, Zhao J (2005) Investigation into micro abrasive intermittent jet machining. *Int J Mach Tool Manu* 45(7-8):873-9.
- [276] Zhang Q, To S, Zhao Q, Guo B (2015) Amorphization and C segregation based surface generation of Reaction-Bonded SiC/Si composites under micro-grinding. *Int J Mach Tool Manu* 95:78-81.
- [277] Zhou G, Yao S-C (2011) Effect of surface roughness on laminar liquid flow in micro-channels. *Appl Therm Eng* 31(2-3):228-34.
- [278] Zhou Y, Axinte D, Butler-Smith P, Jessen E, Norbygaard T (2016) Effects of novel rotary-abrasive finishing pad textures on the controlled 2-body abrasive wear of Type 304 stainless steel. *Wear* 348-349:89-97.
- [279] Zhou Y-F, Wang L, Liu P, Liu T, Zhang L, Huang D-T, Wang X-L (2014) Ridge waveguide fabrication by combining ion implantation and precise dicing on a LiNbO3 crystal. *Nuclear Instruments and Methods in Physics Research Section B: Beam Interactions with Materials and Atoms* 326:110-2.
- [280] Zitt U, Braun O, Warnecke G (1999) Improvement of workpiece quality of ceramic engine valves by kinematic simulation of the valve grinding operation. *Transactions of the NAMARI of SME* 27:153-8.